In presenting the dissertation as a partial fulfillment of the requirements for an advanced degree from the Georgia Institute of Technology, I agree that the Library of the Institute shall make it available for inspection and circulation in accordance with its regulations governing materials of this type. I agree that permission to copy from, or to publish from, this dissertation may be granted by the professor under whose direction it was written, or, in his absence, by the Dean of the Graduate Division when such copying or publication is solely for scholarly purposes and does not involve potential financial gain. It is understood that any copying from, or publication of, this dissertation which involves potential financial gain will not be allowed without written permission.

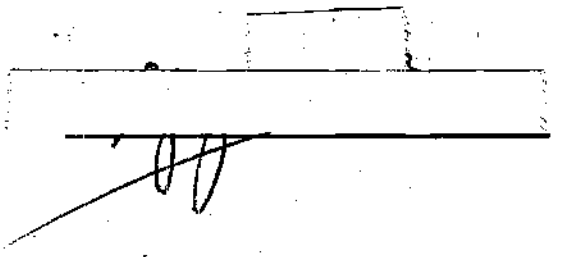

7/25/68

NON-CONDENSABLE GAS DYNAMICS IN THE HEAT PIPE

A Thesis

Presented to

The Faculty of the Graduate Division

by

Gonzalo E. Zevallos

In Partial Fulfillment

of the Requirements for the Degree

Master of Science in Mechanical Engineering

Georgia Institute of Technology

June, 1970

NON-CONDENSABLE GAS DYNAMICS

IN THE HEAT PIPE

Approved:

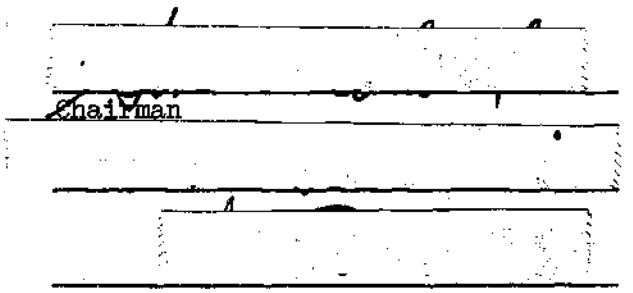

Date approved by Chairman: 6-4-70

ACKNOWLEDGEMENTS

The author would like to express his appreciation to Dr. Gene T. Colwell, his faculty advisor, whose understanding and guidance have made this work possible. The constructive comments and time given by Dr. Novak Zuber and Dr. C. W. Gorton are gratefully acknowledged.

A special note of thanks is due to Mr. C. Lamar Williams who has offered much helpful advice and encouragement during every stage of the research.

Finally, the author would like to express his sincere appreciation to his wife for her continued support and understanding.

TABLE OF CONTENTS

LIST OF TABLES

LIST OF ILLUSTRATIONS

LIST OF ILLUSTRATIONS (Continued)

SUMMARY

The heat pipe is a high heat transport device which uses the evaporation, condensation and surface tension characteristics of a working fluid; it is able to transfer up to 500 times as much heat per unit weight as a solid thermal conductor of equal cross-section (12)*.

Since 1964, heat pipe capabilities and limitations have been extensively studied (1), (6), (17), (20), (21); variations in heat pipe design and operating conditions have been investigated (3), (7), (10), (20), and an engineering theory of heat pipe performance has been proposed (7).

The presence of a non-condensable gas inside a heat pipe affects the performance of the device by reducing the heat transfer rate for a given operating temperature (6), (10), (19). Consequently, the introduction of a predetermined amount of non-condensable gas into the heat pipe could provide an effective means of controlling the heat transfer rates at various operating temperatures.

In the present investigation, a water heat pipe was loaded with various amounts of a non-condensable gas (Argon) in order to investigate the results on heat pipe performance. The rate of heat transfer was found to be significantly reduced, particularly at low vapor temperatures. The reduction in heat transfer was proportional to the amount of Argon introduced.

To account for the reduction in heat transfer, three models were proposed. The first assumed that the gas and the vapor were mixed

*Numbers in parentheses refer to similarly numbered references in the Bibliography.

completely inside the heat pipe; the second model proposed that the gas collected in the condenser forming an annulus at the liquid-vapor interface; finally, the third model assumed that the gas collected at the end furthest from the evaporator forming a slug. Theoretical predictions using each model were compared to the experimental data. The results of these comparisons showed that the first two models did not describe appropriately the phenomena involved. The slug model, however, predicted the reduction in heat transfer with good accuracy. The equation

$$\frac{Q_{nc}}{Q_o} = \frac{(t_{ad}-t_w)_{nc}}{(t_{ad}-t_w)_o}\left(1 - \frac{\frac{P_i T_{ad}}{T_i P_{ad}} L_t - L_x}{L_c}\right)$$

approximates the experimental data with a maximum error of 23 percent and usually much closer than this.

A simplified theoretical analysis of non-condensable gas movement was also made. A mass balance was applied to a system where a gas tends to back-diffuse against the flow of a gas-vapor mixture. The use of experimental data in conjunction with the results of this analysis showed that the tendency of the gas to back-diffuse was opposed by a much larger convective force. This result confirmed the validity of the slug model, where the gas was assumed to be collected at the end of the condenser section of the heat pipe.

By using non-dimensional groups in the analysis of heat pipes, equations suitable for design may be obtained. Figures 26 and 27 are graphs of the non-dimensional groups obtained, relating heat transfer rates to operating temperatures and to gas loading pressures. From Figure 26, the empirical equation

$$\frac{Q}{\sigma r_i (h_{fg})^{\frac{1}{2}}} = (3215 + 25{,}250 \frac{P_i T_{st} L_t}{T_i P_{st} L_c})(\frac{T_{ad} - T_w}{T_{ad}}) -$$

$$(50 + 3900 \frac{P_i T_{st} L_t}{T_i P_{st} L_c})$$

was obtained. Figures 28 through 31 show that this relationship approximates the experimental data very closely.

GLOSSARY OF ABBREVIATIONS

A_c: Condenser area.

A_i: Cross-sectional area ofthe vapor space.

A_l: Cross-sectional area through which liquid flows.

A_v: Available condenser area.

D : Water vapor-Argon mass diffusivity.

d_c: Capillary pore mean diameter.

d_i: Vapor space diameter.

g_c: Gravitational constant = 32.17

h_{fg}: Latent heat of vaporization of the working fluid.

h_i: Heat transfer coefficient for condensing steam.

h_o: Heat transfer coefficient for the cooling water side.

J : Conversion factor = 778

k_{nc}: Thermal conductivity of the non-condensable gas.

k_p: Thermal conductivity of the enclosure.

k_w: Thermal conductivity of the liquid-wick structure.

L_A, L_{nc}: Length of the non-condensable gas slug.

L_c: Length of the condenser section.

L_m: Length of the concave or convex volume.

L_t: Total length of the heat pipe.

L_v: Length of the available condenser area.

L_x: Length of the extended volume.

L_m: Length of the concave or convex volume.

$\mathring{m}$: Mass flow rate of vapor.

m_A: Mass of Argon injected into the heat pipe.

$\dot{m}_w$: Mass flow rate of cooling water.

m_x: Mass of Argon collected in the extended volume.

n_A: Mass of flux of Argon.

n_v: Mass flux of water vapor.

P_{ad}, P_{sat}: Saturation pressure corresponding to t_{ad}.

P_i: Pressure of non-condensable gas inside the heat pipe before water injection (gas loading pressure).

P_{nc}: Pressure of non-condensable gas during operation.

P_{st}: Standard atmospheric pressure.

P_t: Heat pipe total pressure.

P_v: Partial pressure of the water vapor.

Q: Heat transfer, in general.

Q_{nc}: Heat transfer rate with a non-condensable gas included.

Q_o: Heat transfer rate without including a non-condensable gas.

r_A: Inner radius of the Argon annulus.

r_c: Capillary pore mean radius.

r_i: Radius of the vapor space.

r_p: Outer radius of the enclosure.

r_w: Inner radius of the enclosure.

R_{nc}: Argon gas constant.

R_v: Water vapor gas constant.

t_{ad}, T_{ad}: Heat pipe operating temperature.

T_i: Temperature of non-condensable gas inside the heat pipe before water injection.

T_{nc}: Temperature of non-condensable gas during operation.

T_{st}: Standard Temperature.

t_w, T_w: Cooling water average temperature.

U : Overall heat transfer coefficient.

v_l: Liquid axial velocity.

v_v, v_w: Vapor axial velocity.

V_m: Concave or convex volume.

V_{nc}: Volume of the non-condensable gas slug.

V_t: Total volume of the vapor space.

V_x: Extended volume.

W_A: Argon concentration.

W_v: Water vapor concentration.

W_{Ao}: Argon concentration at x = 0.

Subscripts:

nc: With a non-condensable gas included.

o : Without including a non-condensable gas.

CHAPTER I

INTRODUCTION

The Heat Pipe

The heat pipe is a self-contained device capable of transferring large amounts of heat through a very small temperature difference. The common heat pipe consists of an enclosure, usually a long, thin pipe or parallelepiped, lined with a capillary structure along its inside wall. A suitable working fluid saturates the wick with liquid and fills the open section with vapor. Operation of the heat pipe involves adding heat at one end causing the liquid to evaporate; the higher vapor pressure thus created inside the heat pipe drives the vapor towards the opposite end where it condenses by rejecting its latent heat through the wick-pipe structure to a heat sink. The evaporation of the liquid in the evaporator causes the liquid at the interface to retreat into the wick forming a small interfacial radius of curvature; on the other hand, the condensation of vapor results in the formation of a large interfacial radius of curvature in the condenser. This difference in curvature causes the liquid to be pumped by capillary action from the condenser to the evaporator, completing the cycle. See Figure 1.

The heat pipe can be operated over a wide temperature range by an appropriate choice of working fluids. The vapor pressure curve of the fluid dictates the temperature range of applicability. Thus, cryogenic fluids can be used in the very low temperature region (below 200°K);

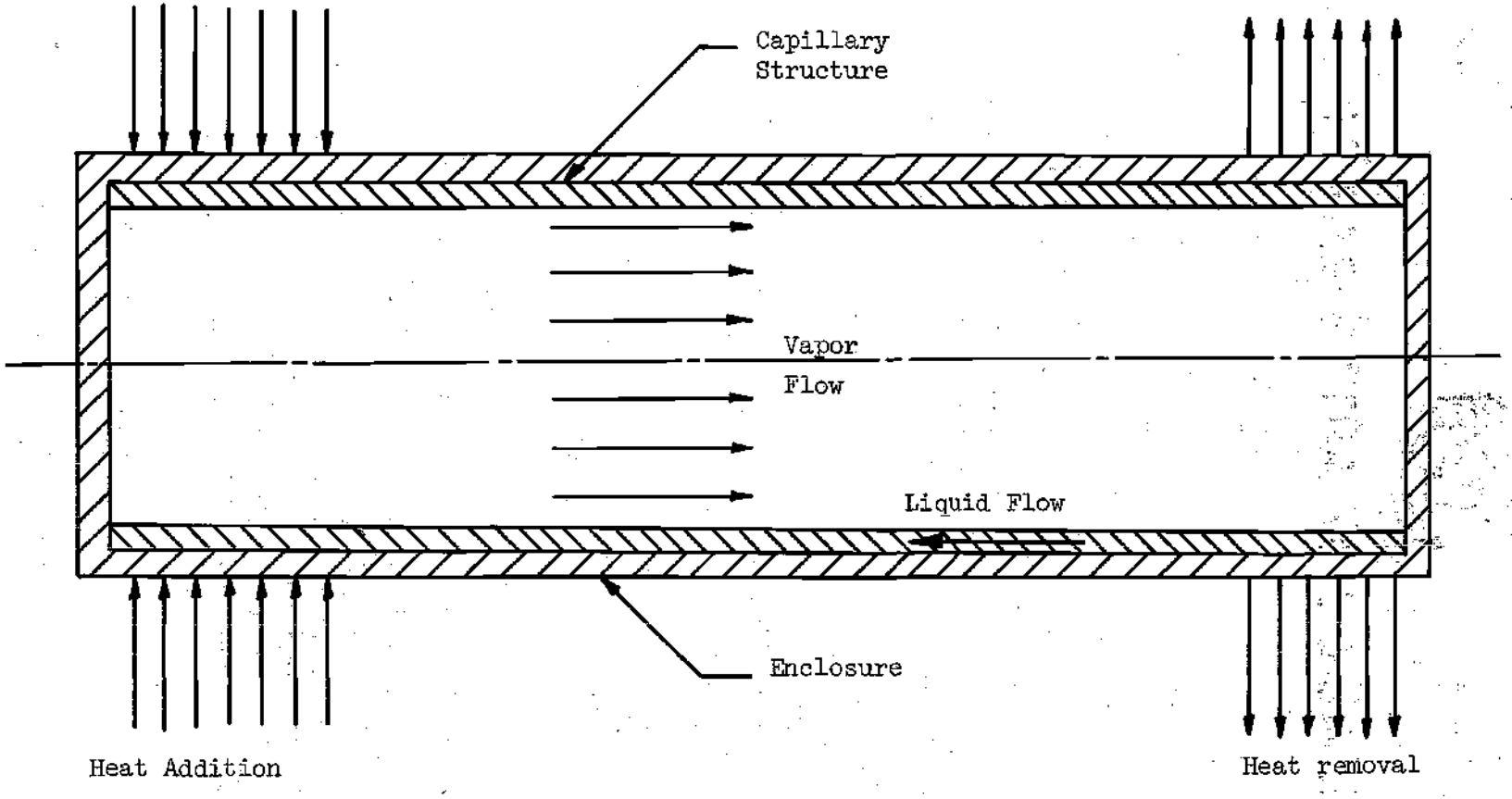

Figure 1. The Ordinary Heat Pipe

ammonia can be used from 200°K to 300°K; water can be used in the range between 300°K and 600°K (1) and liquid metals can be used at high temperatures up to 2300°K (2). Other important fluid properties are latent heat of vaporization, surface tension and wetting ability (3). A high latent heat of vaporization is desirable, since the transport of energy is accomplished by the evaporation and condensation of the working fluid. Consequently the mass flow rate will be small when the latent heat is large. Surface tension and wetting ability are related to the capillary pumping capacity of the liquid-wick structure and they should be high.

The heat pipe has an effective thermal conductivity many times larger than any known material, it has no moving parts and does not depend on the force of gravity for its operation, thus lending itself to many applications, especially in the zero-gravity environment of space.

The amount of heat that can be transferred may be limited by various conditions (4). First, boiling of the liquid may occur in such a way that a vapor film forms at the wick-pipe interface causing a sharp rise in temperature such that burn out of the wick occurs, rendering the heat pipe inoperative. Second, if the capillary pumping is not sufficient to replenish the liquid being evaporated at high heat transfer rates, burn out of the wick will result. Third, given a desired operating temperature, if the heat transfer is such that the vapor velocity reaches the sonic velocity, the vapor pressure and consequently the temperature will rise above desired values. Finally, the shear stress between the liquid in the wick and the counter flowing vapor can increase to such a degree with increasing vapor velocity, that entrainment of the liquid in the vapor may occur.

Statement of the Problem

The purpose of this investigation is to determine the effect of purposely introducing various amounts of a non-condensable gas (Argon) in the vapor space of a water heat pipe. It is a conjectured that the rate of heat transfer for a given operating temperature will be reduced. The possible mechanisms of heatreduction are to be studied and compared with experimental data, such that analytical equations suitable for heat pipe design can be obtained.

The variables affecting heat pipe performance are to be grouped into non-dimensional quantities and these quantities correlated so as to obtain generalized performance curves. Finally, a simplified theoretical analysis of gas movement is to be made, thus predicting the convective and diffusive flow of the non-condensable gas and its distribution inside the heat pipe as a function of the operating variables.

This investigation, therefore, is concerned with the possibility of using a non-condensable gas as a means of varying the operating characteristics of a heat pipe such that it can be made to operate over a wider range of heat transfer rates and temperatures.

Literature Survey

The concept of the heat pipe originated with R. Gaugler (5) who, in 1944, obtained a patent for a heat transfer device that used the evaporation and condensation of a volatile liquid at essentially the same pressure. The system was a closed one and the flow of liquid from condenser to evaporator was accomplished by capillary action.

The heat pipe was rediscovered by Grover, et al (6) in 1964. They

constructed and studied several heat pipes utilizing water and sodium as working fluids. Measurements of heat transfer rates and operating temperatures were made. Maximum heat fluxes of about 30 watts/cm^2 were reached with a sodium heat pipe before failure occurred. They attributed the failure to drying of the wick. A region of rapidly decreasing temperature was observed at the cool end of the heat pipe. The authors speculated that this was due to the presence of hydrogen gas, a common impurity in sodium metal.

Cotter (7) in 1965 developed the first engineering theory for heat pipe design and performance analysis. His study indicated that heat transfer rates are limited by the ability of the wick to pump the liquid to the heated section and by the possibility of boiling occurring at the wick-enclosure interface.

In 1967, Cosgrove (8) made an analytical study of heat pipe operation. His model was based on fundamental heat, mass and momentum balances in the wick, assuming that capillary action was the controlling factor in heat pipe performance. The analysis predicted the maximum heat input as a function of fluid and wick characteristics and the angle of inclination of the heat pipe with respect to gravity. Experiments using a water heat pipe were conducted and the results compared to the predictions of the analytical model. The agreement was good.

Numerous variations of heat pipe design have been investigated. Different geometries have been used, the preferred ones being the long thin pipe (7), (8), (9) and the "box" (10). The influence of working fluid on heat pipe performance has also been studied (1), (3), (11); the most commonly used working fluids have been liquid metals (12), (13) and

water (14), (15). Several types of wick configurations have been used, namely, grooves in the pipe wall (16), packed beads (17), various layers of screen (18), (19), and sintered metals (20).

Various aspects of heat pipe operation have been investigated. The heat transfer limitations of heat pipes, as explained in Chapter I and its causes have been extensively studied (1), (17), (20), (21), (22). Temperature gradients along the heat pipe have been measured (17), (23) and pressure drops in the vapor space calculated (24). Vapor and liquid velocities have been predicted theoretically (25), (26).

The heat pipe is amenable to many practical applications. Several authors (2), (27), (28), (29), (30) have suggested a number of them for space and ground use.

The presence of non-condensable gases inside the heat pipe was first noted by Grover et al. (6) as mentioned above, but they did not study the possible effects of its presence on overall performance.

In a later publication, dealing with heat pipe start-up dynamics, Cotter (31) stated that "as the vapor pressure increases, non-condensable gas is swept out of the evaporator region until pressure in the vapor and gas are equal and a well defined interface is formed between the two. As the vapor pressure increases with further increase in temperature, the vapor zone increases in length, sweeping the non-condensable gas before it and compressing it into the cold terminal end of the pipe."

Kunz, et al. (10) conducted a study of heat pipe temperature distributions and limiting heat fluxes using the "box" configuration and water as working fluid. The results of tests run with nitrogen gas present in the vapor space, showed that the heat pipe remained essentially

isothermal. The authors concluded that the gas and the vapor were thoroughly mixed during operation. This could have been caused by the large difference in molecular weight of the two fluids and the large passage cross-sectional area, both of which aid in the diffusion of the gas throughout the vapor space. Theoretical predictions of the operating pressure for the cases of mixing and no mixing were compared with the experimental values. The results confirmed that the gas and the vapor were probably mixed.

Anand, et al. (19) related the optimization of a heat pipe to condenser parameters. They suggest that the heat transfer characteristics may be varied by the introduction of a non-condensable gas, but offer no further insight into the problem.

The use of stainless steel wicks and water as a working fluid results in the formation of hydrogen gas as reported by Schwartz (32). Water and water-ammonia heat pipes were operated for several days. The presence of the hydrogen gas after the first few days was evident because of a significant temperature difference between the ends of the heat pipe. The authors attributed this temperature drop to the formation of an annular layer of gas in the terminal end of the condenser, such that it prevented the normal condensation of vapor, removing that portion of the condenser from the heat-pipe loop.

In 1968, Lee and Werner (4) designed a "gas buffered annular heat pipe fuel irradiation capsule," to meet the requirements of handling "large and varying fuel specimen heat fluxes while inherently maintaining nearly constant specimen temperature." Tests using sodium and potassium as working fluids were performed. The temperature readings indicated

that the gas collected at the end of the condenser section and that a distinct interface existed between the gas and the vapor. This interface seemed to move, compressing the gas against the terminal end with increasing power input.

Werner (33) has suggested the use of lithium heat pipes as a means of regenerating tritium to maintain cycle continuity in thermonuclear reactors using the D-T reaction. The heat pipe is located in a neutron environment (in the blanket of a thermonuclear reactor) such that tritium is produced by nuclear reaction. This tritium will be transported to the end of the condenser where it will collect and a distinct interface will form between it and the flowing vapor. Back diffusion of the tritium gas was shown to be unlikely due to the large vapor velocities (0.5 x sonic velocity). Molybdenum was used as the pipe material, and the tritium was recovered as it diffused through the pipe wall.

CHAPTER II

EQUIPMENT

The heat pipe used in this research was constructed using a 304 stainless steel tube of 0.730 inch outside diameter and 0.622 inch inside diameter. The capillary structure consisted of two layers of 100 mesh 304 stainless steel screen. The structure was insulated with asbestos insulation to minimize heat losses to the surroundings; see Figure 2. The total length of the heat pipe was 20.25 inches; energy was supplied along a 3.25 inches long evaporator and removed along a condenser section 6.00 inches long; the heat pipe also included an adiabatic section 8.75 inches long and an extended volume beyond the condenser whose length was estimated to be 2.25 inches; see Figure 3. Separate ports were provided for the injection of water and argon and a third port was connected to a vacuum system.

Argon was supplied from a pressurized container. The amount supplied was monitored by reading pressure with an Alphatron* vacuum gage and temperature with thermocouples. The water injection system consisted of a graduated burette wrapped with an electric heating element such that unaccountable non-condensable gases could be boiled out of the water before injection; a needle valve was used to aid in accurately metering of the water used as a working fluid (20 milliliters).

Heat was supplied to the heat pipe by an electric resistance coil wrapped onto a hollow ceramic core and positioned along the evaporator

*Trade Mark NRC Equipment Corporation.

section. The electrical supply system consisted of a variable autotransformer, a voltmeter and an ammeter, all rated at 20 amps. The heat removal was accomplished by passing cooling water through a concentric water jacket in the condenser section. The vacuum system consisted of a small vacuum pump, connecting steel piping, vacuum needle valves, and a thermocouple vacuum gage.

Four copper-constantan thermocouples were silver soldered to the heat pipe along the adiabatic section at 2 inches intervals. The average of the reading of thermocouples five and six (see Figure 3) was used as the operating temperature of the heat pipe. In addition, thermocouples were placed at the inlet and outlet ports of the cooling water jacket. Cooling water flowed from a constant head source through the jacket and was collected in a graduated cylinder. A differential pressure transducer was used to measure the heat pipe pressure. The excitation voltage for the transducer was provided from a D.C. power supply. Doubts in the reliability of the pressure measurements were caused by difficulty encountered in trying to keep this power supply at a constant setting. A recorder was used to monitor the readings of the heat pipe thermocouples and the pressure transducer. The difference in readings between the cooling water jacket thermocouples was read directly on a potentiometer. In addition, the Alphatron vacuum gage was used to measure the Argon loading pressure. Figure 4 shows a schematic diagram of the equipment arrangement.

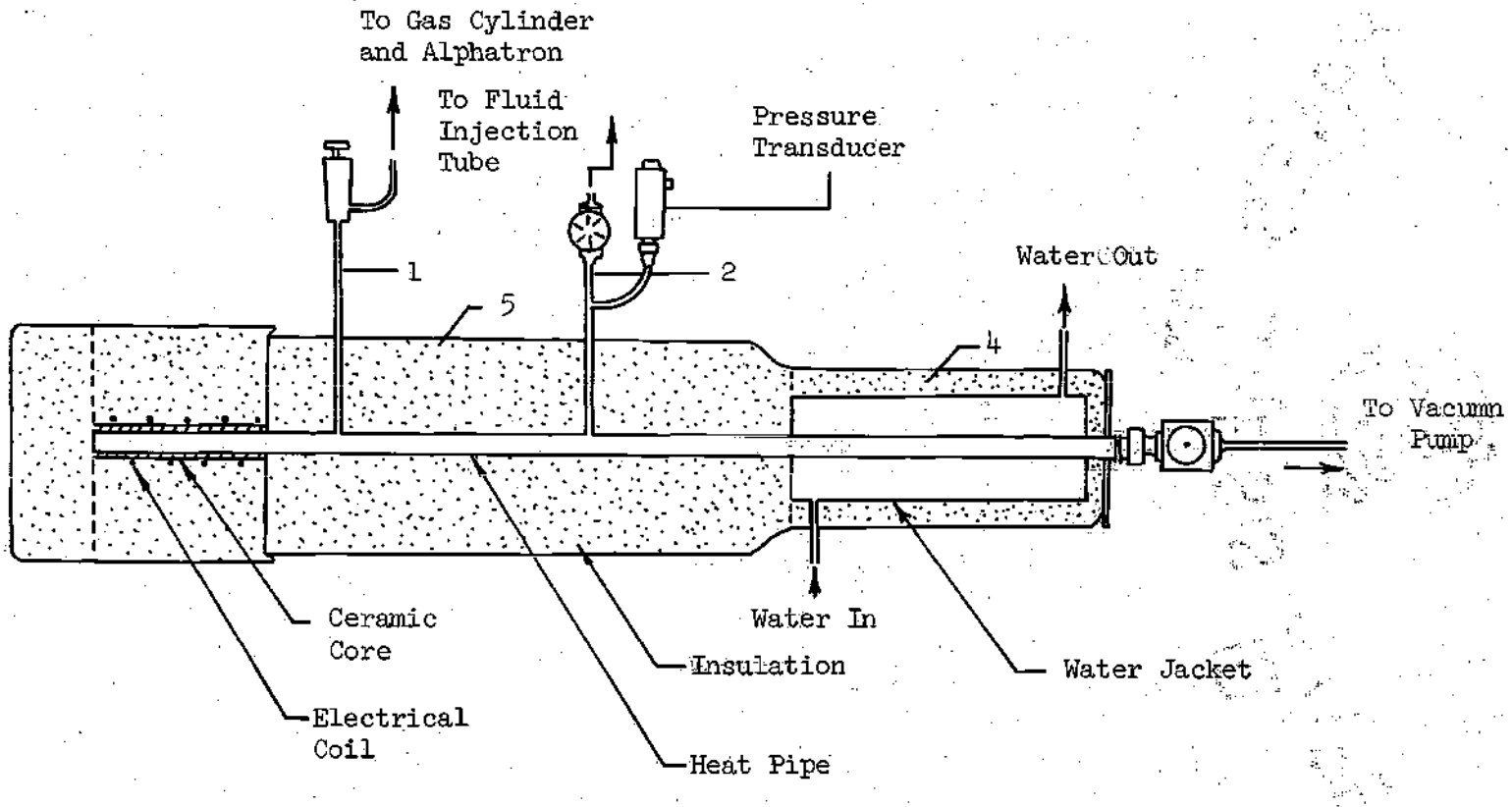

Figure 2. Heat Pipe and Connections

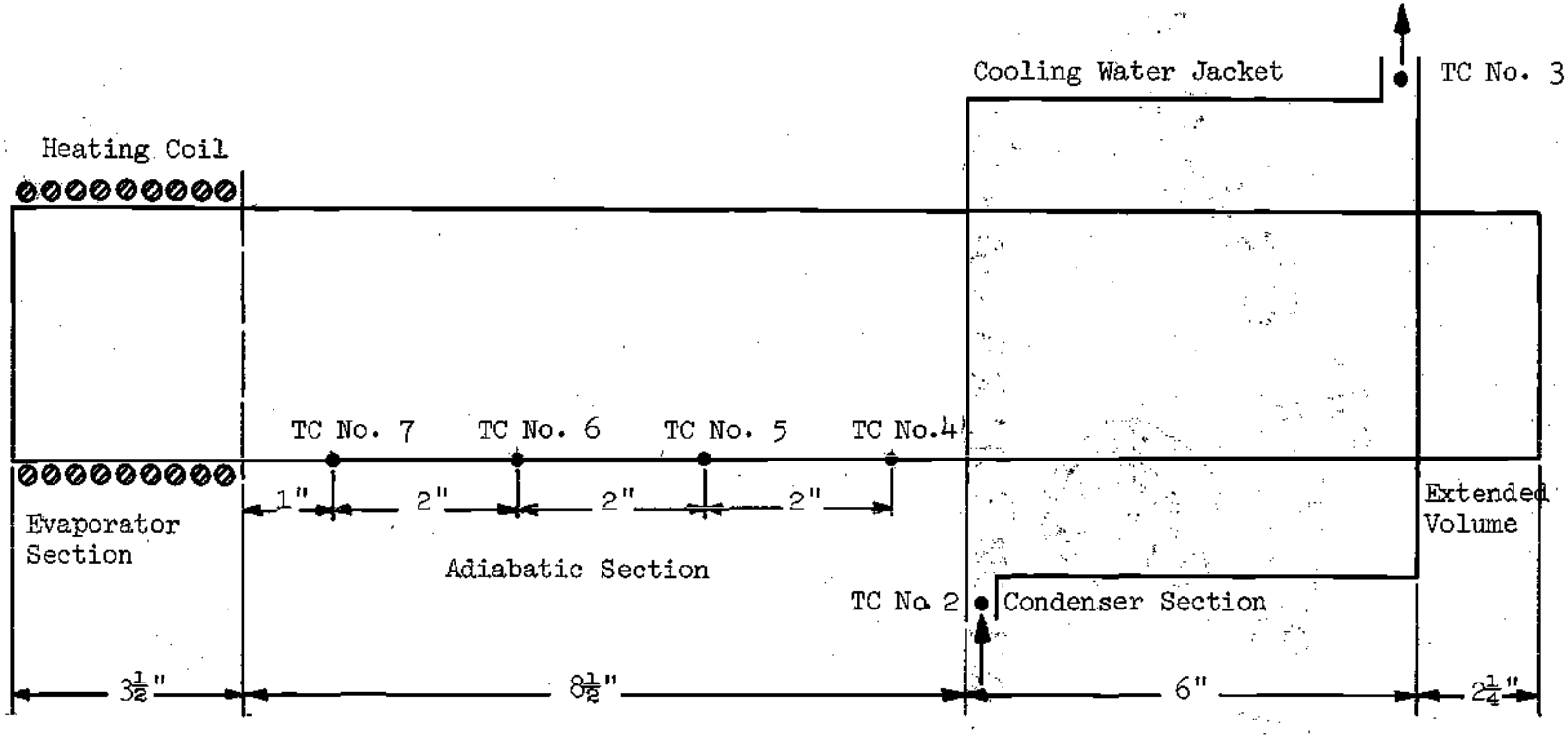

Figure 3. Sections of the heat pipe and location of thermocouples.

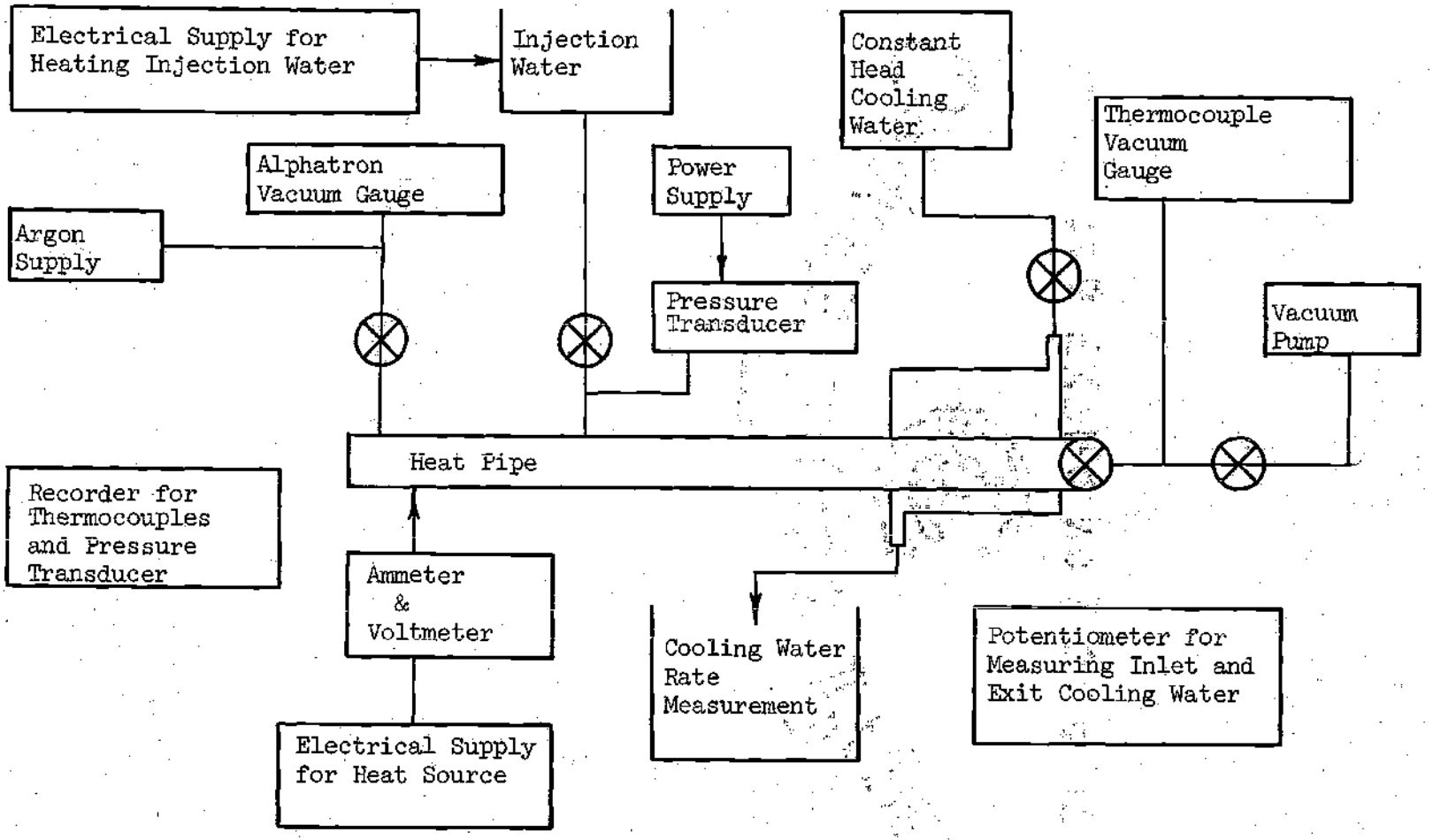

Figure 4. Equipment Schematic

CHAPTER III

PROCEDURE

The steps to be followed in preparation for, and during each run are outlined below.

1. The test section is cleaned and assembled with the heat pipe in the horizontal position.

2. The heat pipe is connected to the vacuum system and pumped until the pressure stabilizes at about one micron of Hg.

3. All valves are closed and the system is monitored with the thermocouple vacuum gage to check for leaks. If the observable pressure rise is less than five microns of Hg per hour, the system is assumed to be leak tight for the purposes of this investigation.

4. A predetermined amount of Argon is slowly bled into the heat pipe and all valves are closed until the system comes to thermal equilibrium. The pressure and temperature inside the heat pipe are recorded.

5. Distilled water, to be used as the working fluid, is boiled in a calibrated burette to remove absorbed gases and then slowly bled into the heat pipe in two 10 ml. portions.

6. Cooling water is then allowed to flow from a constant head source through the cooling jacket. The flow rate of the cooling water is adjusted by use of a valve and measured by collecting the flow in a graduated cylinder over a measured time interval. A constant flow of 0.515 liters/min is used throughout these experiments.

7. Next, the evaporator heating coil is turned on to a power setting of 20 volts. The temperatures in the adiabatic region and the operating pressure are observed in the monitoring recorder during the heating phase. Once steady state conditions have been reached, measurements are made of the cooling water flow rate and temperature rise of the cooling water in passing through the jacket. These are recorded together with readings of the thermocouples in the adiabatic section and reading of the pressure transducer.

8. The power setting is then increased to the next desired level and the procedure followed in step 7 is repeated. A maximum power setting of 68.5 volts is used in these tests and the power settings are usually changed in increments of 10 volts.

9. When the run is completed the electric power and the cooling water are turned off and the system is allowed to cool to room temperature. At the end of the cooling period the final pressure in the heat pipe is read and recorded.

10. The pipe is then connected to vacuum system which pumps all water and gases from the heat pipe in preparation for the next run.

Heat pipe pressures and temperatures range from 1 inch to 20 inches Hg and 70° to 180°F, respectively, while heat rates vary between 0 and 1100 Btu/hr. Non-condensable gas loading pressures vary between 0.0 and 2.0 inches Hg with the working space evacuated before injection of Argon.

CHAPTER IV

OVERALL EFFECT OF THE PRESENCE OF A NON-CONDENSABLE GAS IN THE HEAT PIPE

Experimental Results

Figure 5 shows curves of the heat transfer rates through the condenser versus the operating temperatures, for different Argon loading pressures.

The apparent effect of the presence of a non-condensable gas inside the heat pipe is a reduction in the rate of heat transfer. An attempt to explain the mechanism by which this reduction in heat transfer rate occurs will be made in the next section.

From these curves it can be seen that for increasing amounts of gas, the reduction in heat transfer is proportionately larger. One noteworthy aspect of these curves, is that, regardless of the amount of Argon originally injected, as the operating temperature increases all curves approach the no non-condensables curve; this is partly due to the presence of the extended volume at the condenser. As the temperature, and consequently the operating pressure of the heat pipe increases, the Argon is forced into this extended volume thus exposing more of the condenser surface. By imagining the gas to be accumulated at the condenser end (a fact that was later confirmed by empirical and analytical modeling) the amount of gas present inside the actual heat pipe (that is, not including the extended volume) can be calculated and curves of heat transfer

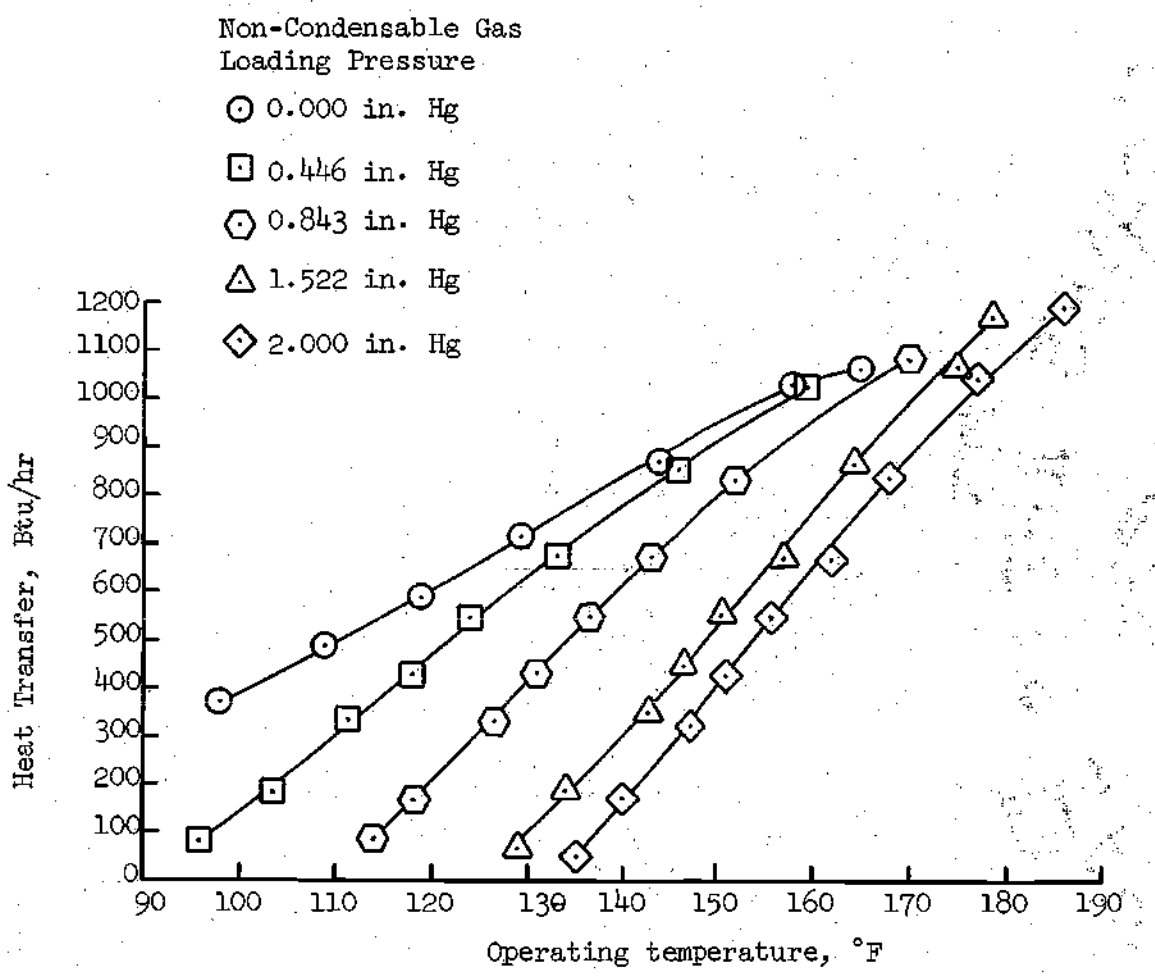

Figure 5. Heat transfer rates vs. operating temperature

rate versus operating temperature for various amounts of gas can be obtained. Figure 6 shows these curves which seem to confirm the idea that by varying the amount of gas included in the heat pipe, the position and the slope of the curves, and therefore the operating characteristics of the heat pipe, could be controlled at will, within a certain range. Also included is a plot of heat transfer rate versus the mass inside the actual heat pipe for various operating temperatures (Figure 7).

In Figure 8 a plot of Q_{nc}/Q_o (the ratio of heat transfer rate with a gas present inside the heat pipe to the heat transfer rate with no gas present) versus the initial gas loading pressure for various operating temperatures is shown. Here, again, it can be seen that the heat transfer rate decreases with increasing amounts of non-condensable gas present inside the heat pipe. Finally, Figure 9 confirms that the reduction is greater for higher gas loading pressures and also that the effect of increasing the operating temperature is that of reducing the effects due to the presence of the gas.

Modeling

It is intended in this section to model the behavior of the non-condensable gas in the heat pipe and derive, from these models, equations that would predict the reduction in the heat transfer rate due to the presence of the gas. Three such models are proposed and discussed below. The approach used is based on a similar analysis used in reference (10).

Mixing of Vapor and Non-Condensable Gas

This model assumes that the non-condensable gas and the vapor are

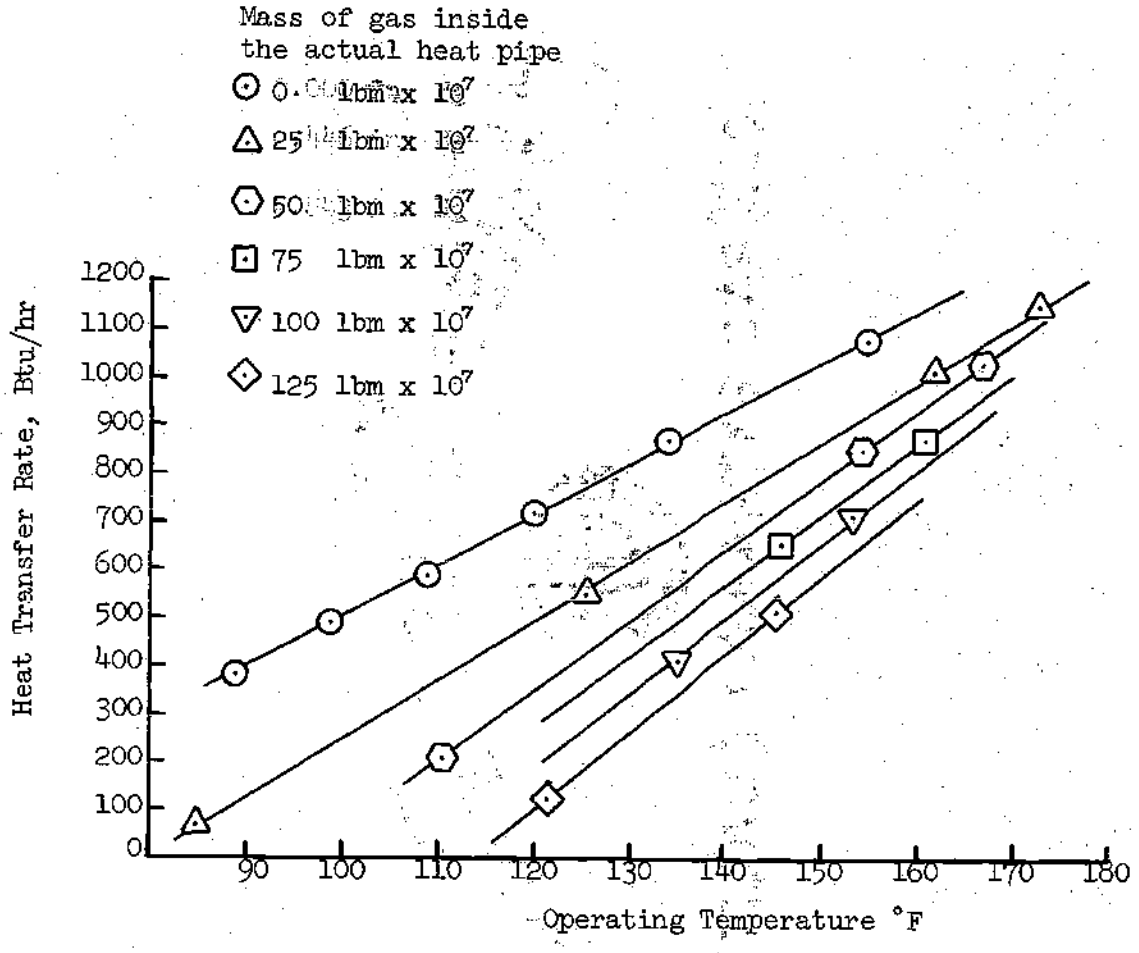

Figure 6. Heat transfer rates vs. operating temperature

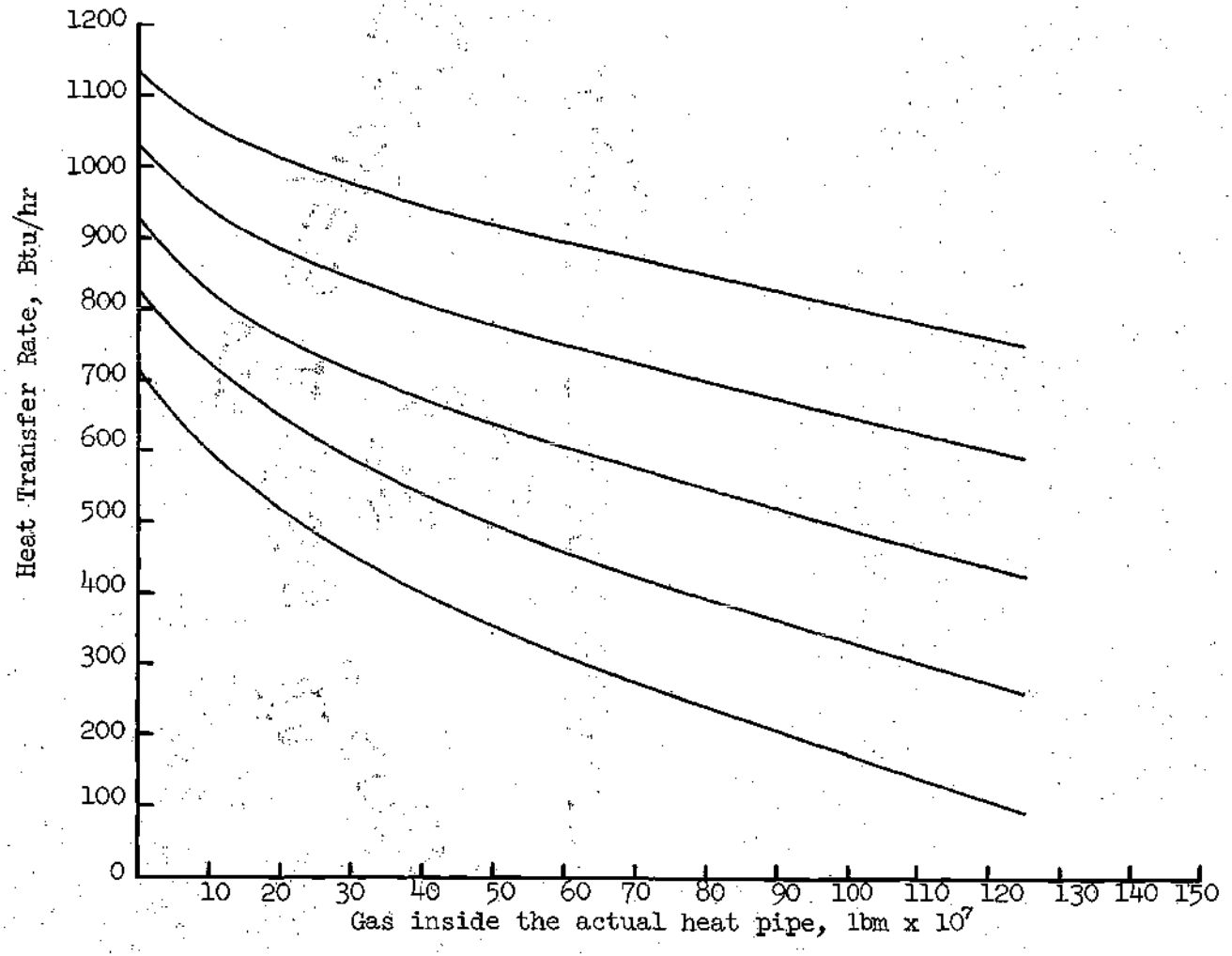

Figure 7. Heat Transfer Rate vs. Mass of Gas Inside the Actual Heat Pipe

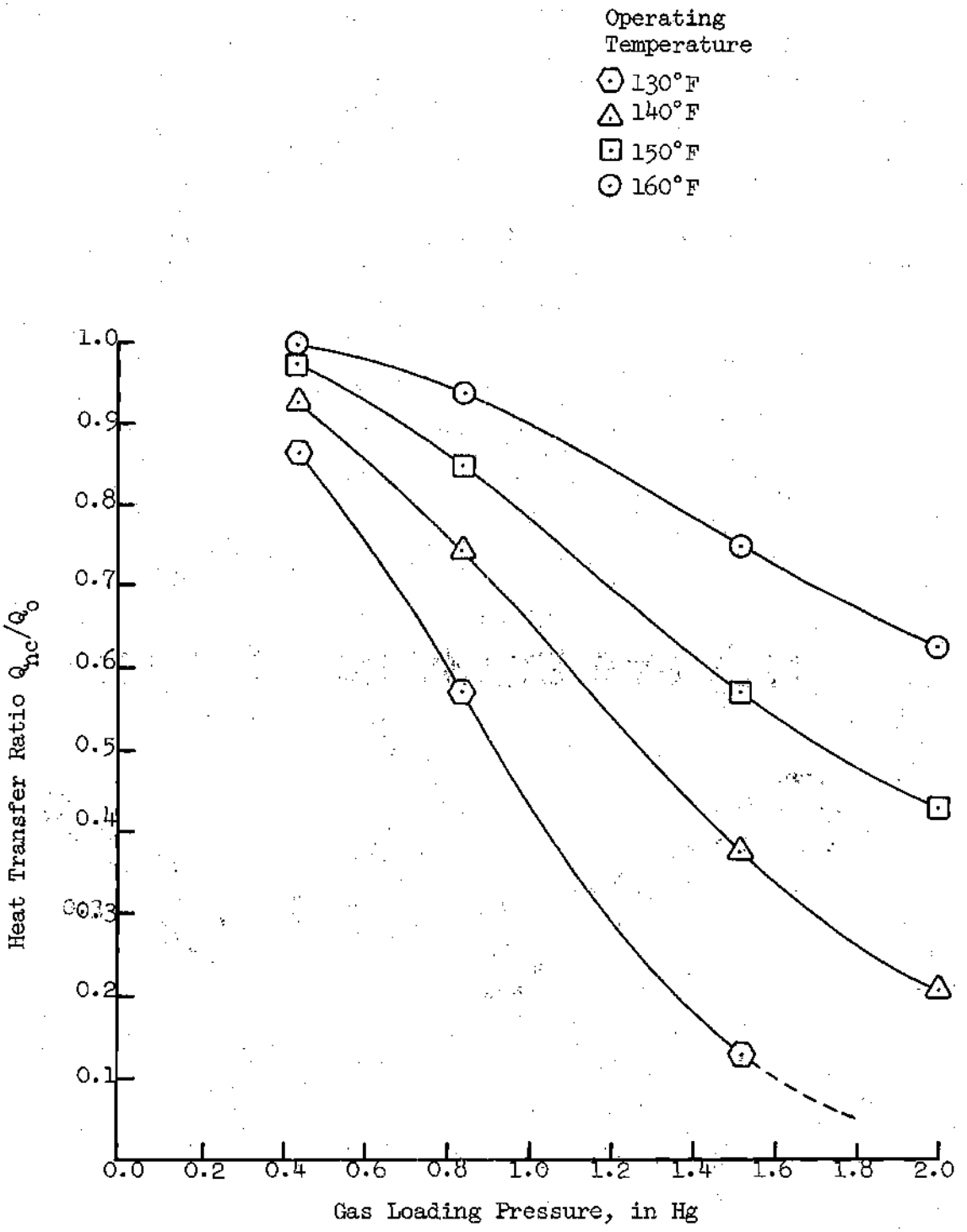

Figure 8. Heat Transfer Ratio $\frac{Q_{nc}}{Q_o}$ vs. Gas Loading Pressure

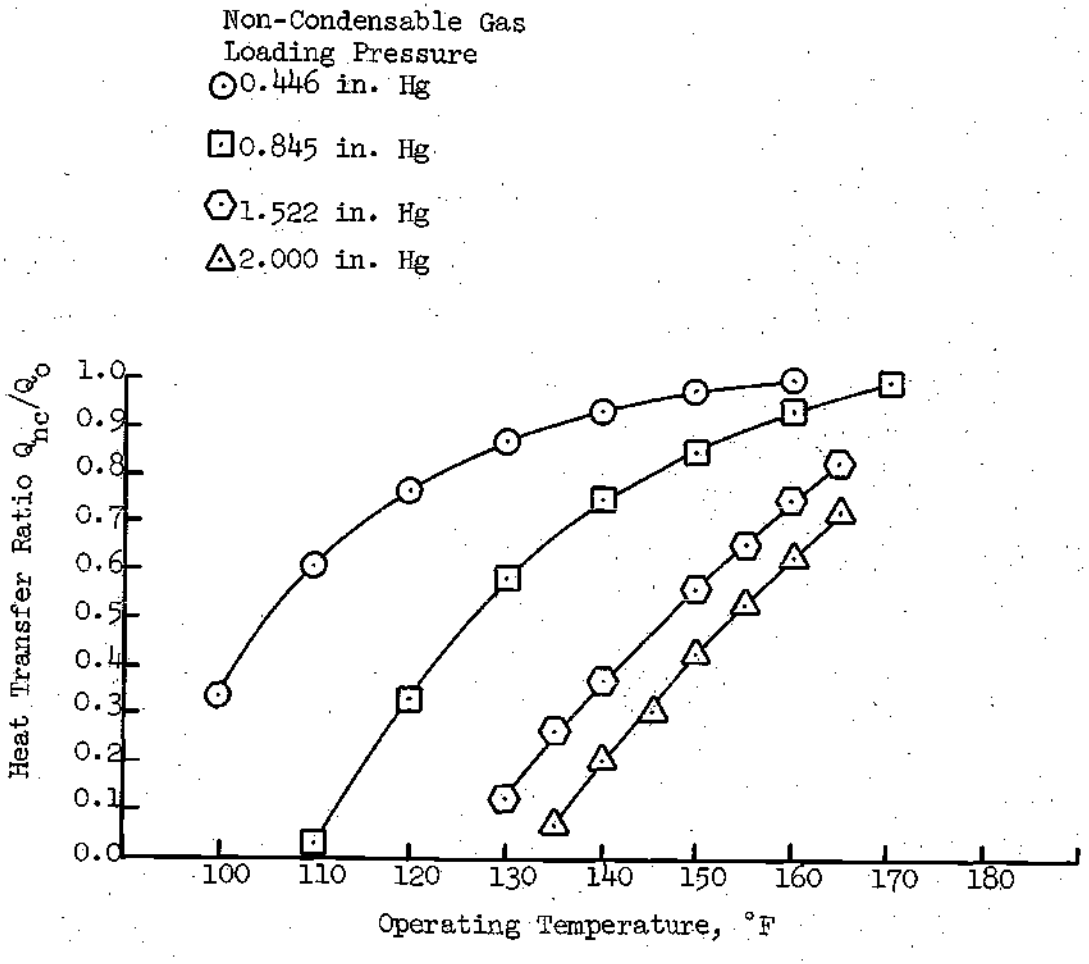

Figure 9. Heat Transfer Ratio Q_{nc}/Q_o vs. Operating Temperature

mixed throughout the vapor space of the heat pipe. Some vapor molecules flowing towards the condenser collide with the non-condensable gas particles producing a reduction in vapor mass flow rate and consequently a lower heat transfer rate. A simple calculation, however, will show that for the heat pipe used in these experiments the mixing model does not apply. The partial pressure of the non-condensable gas can be expressed as

$$P_{nc} = \frac{P_i \, T_{ad}}{T_i} \qquad (1)$$

However, the partial pressure of the gas can also be obtained from the difference between the total pressure of the heat pipe and the partial pressure of the vapor; which is saturation pressure corresponding to the operating temperature.

Tables 1 and 2 show some results of these calculations. There seems to be no apparent relationship between the two sets of values calculated for P_{nc}. This leads to the conclusion that the two phases are probably not mixed throughout the vapor space.

Annulus Model

This model assumes that, when the heat pipe is in operation, the vapor and the gas do not mix, but the gas, carried by the vapor flow, collects at the liquid=vapor interphase in the condenser forming an annulus as shown in Figure 10. The thickness of the annulus, as calculated from equation (9) below is of the order of 0.1 inches so that heat is transported across it mainly by conduction. It is assumed that the vapor condenses on the inner surface of this annulus and that the liquid subsequently finds its way into the wick, Thus, the heat transfer rate is

Table 1. Non-Condensable Gas Partial Pressures, Mixing Model, Run 13

Operating temperature t_{ad}, °F	Heat pipe Total Pressure P_t, in. Hg	Vapor Saturation Pressure P_{ad}, in. Hg	Non-Condensable Gas Partial Pressure $P_{nc} = P_t - P_{ad}$	Non-Condensable Gas Partial Pressure $P_{nc} = \frac{P_i T_{ad}}{T_i}$
96	2.4	1.7	0.7	0.5
104	2.9	2.2	0.7	0.5
112	3.8	2.7	1.1	0.5
118	4.6	3.3	1.3	0.5
124	5.3	3.8	1.5	0.5
133	6.4	4.9	1.5	0.5
146	9.2	6.9	2.3	0.5
160	12.2	9.7	2.5	0.5

Table 2. Non-Condensable Gas Partial Pressures, Mixing Model, Run 16

Operating temperature t_{ad}, °F	Heat pipe Total Pressure P_t, in. Hg	Vapor Saturation Pressure P_{ad}, in. Hg	Non-Condensable Gas Partial Pressure $P_{nc} = P_t - P_{ad}$	Non-Condensable Gas Partial Pressure $P_{nc} = \frac{P_i T_{ad}}{T_i}$
140	6.0	5.9	0.1	2.3
147	7.8	7.0	0.8	2.3
151	8.5	7.8	0.7	2.3
156	10.0	8.8	1.2	2.3
162	12.0	10.1	1.9	2.3
168	14.0	11.6	2.4	2.4
177	18.0	14.7	3.7	2.4
185	20.4	17.1	3.3	2.4

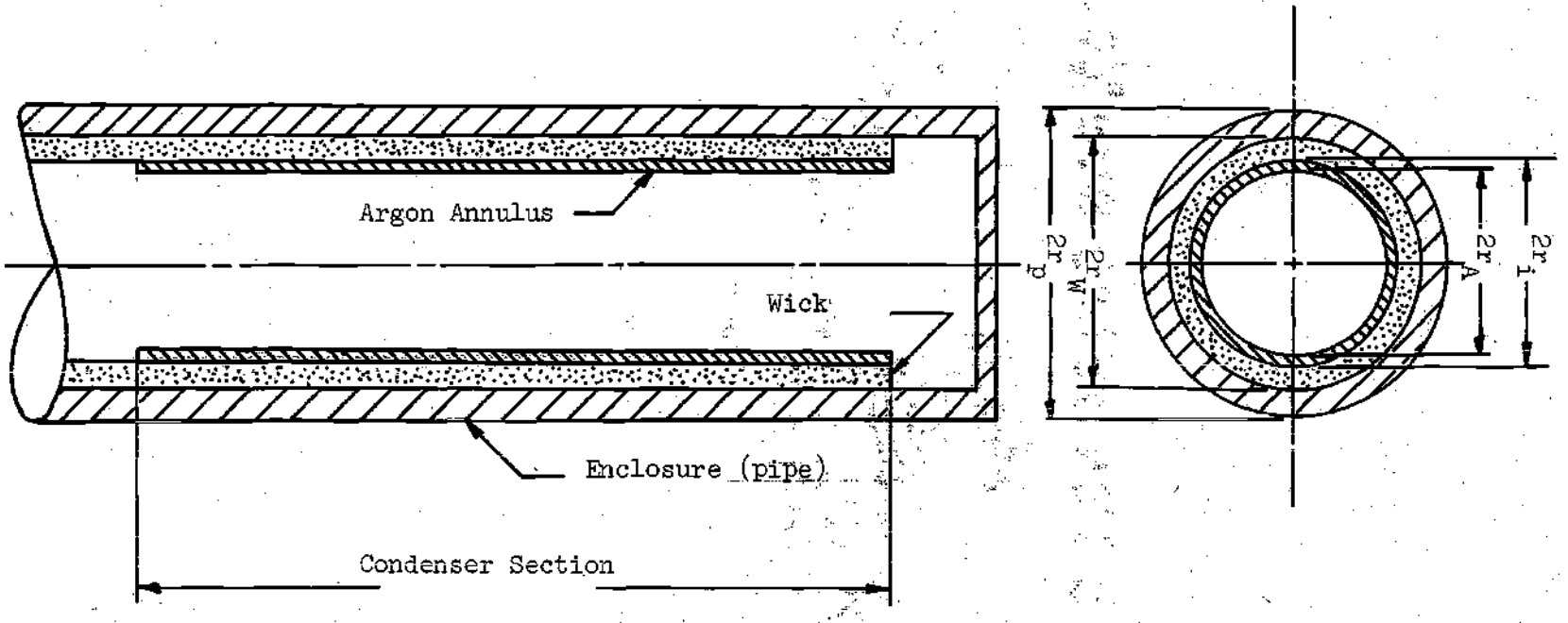

Figure 10. Annulus Model

reduced by the inclusion of an additional thermal resistance. Additional assumptions are:

1) Uniform pressure throughout the vapor space. This seems to be the mode of operation of the heat pipe as substantiated by previous reports (7), (8), (9).

2) Uniform vapor temperature. The observed temperature rise is always small, ranging from 1°F to about 15°F (17), (13) which justifies this assumption.

3) Cooling water temperature assumed constant at an average value. The heat transfer rate when there is no gas included can be expressed as

$$Q_o = U_o(2\pi r_p L_c)(t_{ad}-t_w)_o \tag{2}$$

and when a non-condensible gas is present, as

$$Q_{nc} = U_{nc}(2\pi r_p L_c)(t_{ad}-t_w)_{nc} \tag{3}$$

Therefore:

$$\frac{Q_{nc}}{Q_o} = \frac{U_{nc}}{U_o}\,\frac{(t_{ad}-t_w)_{nc}}{(t_{ad}-t_w)_o} \tag{4}$$

Now:

$$\frac{1}{U_o} = \frac{r_p}{r_i}\frac{1}{h_i} + \frac{r_p \ln r_w/r_i}{k_w} + \frac{r_p \ln r_p/r_w}{k_p} + \frac{1}{h_o}$$

and

$$\frac{1}{U_{nc}} = \frac{r_p}{r_A}\,\frac{1}{h_i} + \frac{r_p \ln r_i/r_A}{k_{nc}} + \frac{r_p \ln r_w/r_i}{k_w} + \frac{r_p \ln r_p/r_w}{k_p} + \frac{1}{h_o}$$

combining these two expressions and after some manipulation:

$$\frac{U_{nc}}{U_o} = \frac{1}{1 + \frac{U_o r_p}{k_{nc}} \ln r_i/r_A + \frac{U_o r_p (r_i - r_A)}{h_i r_i r_A}} \tag{5}$$

But from an order of magnitude analysis:

$U_o \approx 3 \times 10^2$ btu/hr-ft^2-°F, obtained from the experimental data of test No. 9 as $U_o = Q_o/A(t_{ad} - t_w)_o$ by taking an average value over the whole range of operation.

$r_A \approx 1.7 \times 10^{-2}$ ft, obtained from equation (9) below.

$r_p \approx 3 \times 10^{-2}$ ft, from the pipe dimensions.

$r_i \approx 2 \times 10^{-2}$ ft, from heat pipe dimensions.

$k_{nc} \approx 1 \times 10^{-2}$ btu/hr-ft-°F (34).

$h_i \approx 3 \times 10^4$ btu/hr-ft^2-°F (35).

So

$$\frac{U_o r_p}{k_{nc}} \ln r_i/r_A \approx 1.4 \times 10^2, \text{ and}$$

$$\frac{U_o r_p (r_i - r_A)}{h_i r_i r_A} \approx 4.5 \times 10^{-3}$$

Therefore the last term in the denominator may be neglected, and

$$\frac{Q_{nc}}{Q_o} = \frac{(t_{ad} - t_w)_{nc}}{(t_{ad} - t_w)_o} \times \frac{1}{1 + \frac{U_o r_p}{k_{nc}} \ln r_i/r_A} \tag{6}$$

The ratio r_i/r_A is found as follows. When the Argon is injected

it occupies the whole vapor space, so:

$$P_i V_t = m_A R_{nc} T_i, \text{ or}$$

$$P_i(\pi r_i^2 L_t) = m_A R_{nc} T_i \tag{7}$$

At operating conditions, if it is assumed that the average Argon temperature differs only slightly from the vapor saturation temperature:

$$P_{ad}\pi(r_i^2 - r_A^2)L_c = m_A R_{nc} T_{ad} \tag{8}$$

From equations (7) and (8)

$$r_A = r_i \left(1 - \frac{P_i T_{ad} L_t}{T_i P_{ad} L_c}\right)^{\frac{1}{2}} \tag{9}$$

The values of Q_{nc}/Q_o predicted by equation (6) are found to be two orders of magnitude smaller than the experimental values. Even though there are many simplifying assumptions imposed on this model, the magnitude of the difference between experimental and predicted values seems to indicate that the Argon does not behave in the way presuposed by the annular model.

Slug Model

This model assumes that the non-condensable gas is carried by the bulk flow of vapor towards the condenser end and is accumulated at that end forming a slug as shown in Figure 11.

Assume:

1) Uniform pressure inside the heat pipe, equal to the vapor saturation pressure.

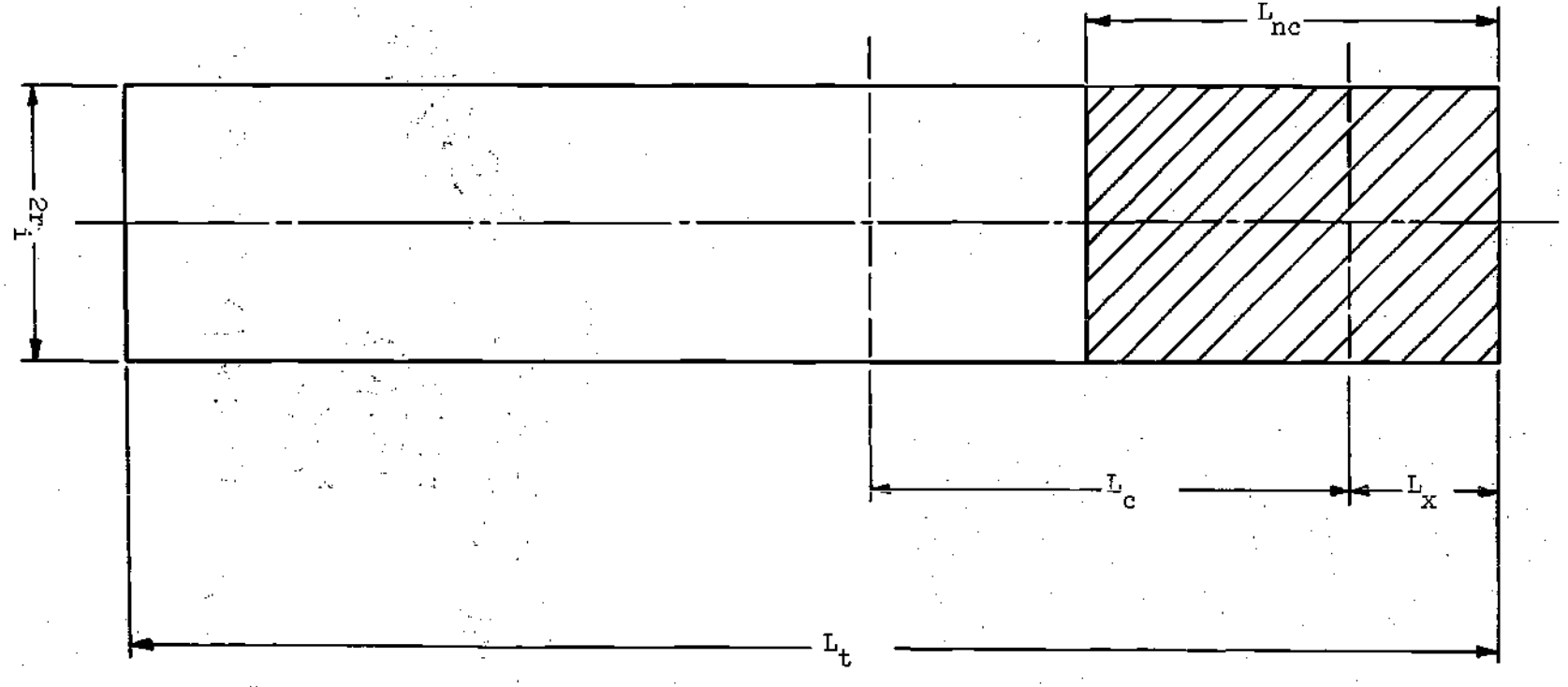

Figure 11. Slug Model

2) Uniform non-condensable gas temperature, equal to the operating temperature of the heat pipe. This is not exactly true; actually, a temperature gradient exists across the non-condensable gas. Even though information relative to this temperature drop in a water heat pipe is scarce, the data of Schwartz (32) seems to suggest that the maximum temperature drop is about 30°R, making the average gas temperature about 15°R lower than the vapor temperature. In the range of operation used in our experiments this would mean that a maximum error of about 2.7 percent is made in assuming the gas to be at the vapor temperature.

3) Heat transfer through non-condensable gas is negligible. The thermal resistance of the non-condensable gas is so large, that if we assume no penetration of the gas by the vapor, the amount of heat transferred through the gas is extremely small.

4) Cooling water temperature can be assumed constant at the average value between inlet and exit temperatures.

5) The overall heat transfer coefficient remains unchanged for the same operating temperature.

This model predicts that the reduction in heat transfer is accomplished by a reduction in the effective condenser area.

The heat transfer rate when no non-condensables are present can be expressed as:

$$Q_o = UA_c(t_{ad}-t_w)_o \tag{10}$$

When a non-condensable gas is injected, for the same operating temperature:

$$Q_{nc} = UA_v(t_{ad}-t_w)_{nc} \tag{11}$$

Therefore:

$$\frac{Q_{nc}}{Q_o} = \frac{A_v(t_{ad}-t_w)_{nc}}{A_c(t_{ad}-t_w)_o} - \frac{L_v}{L_c}\frac{(t_{ad}-t_w)_{nc}}{(t_{ad}-t_w)_o} \tag{12}$$

Now, for the non-condensable gas,

$$P_{nc}V_{nc} = m_A R_{nc} T_{nc}, \text{ or}$$

$$P_{nc}\pi r_i^2 (L_{nc} + L_x) = m_A R_{nc} T_{nc}; \text{ so}$$

$$L_{nc} = \frac{m_A R_{nc} T_{nc}}{\pi r_i^2 P_{nc}} - L_x \tag{13}$$

Before the water is injected, the Argon occupies the whole vapor space, thus,

$$P_i V_t = m_A R_{nc} T_i, \text{ or}$$

$$m_A R_{nc} = \frac{P_i \pi r_i^2 L_t}{T_i} \tag{14}$$

Substituting into equation (13) and recalling that $P_{nc} = P_{ad}$ and that $T_{nc} = T_{ad}$,

$$L_{nc} = \frac{P_i T_{ad}}{T_i P_{ad}} L_t - L_x \tag{15}$$

But

$$L_v = L_c - L_{nc} = L_c\left(1 - \frac{\frac{P_i T_{ad}}{T_i P_{ad}} L_t - L_x}{L_c}\right) \tag{16}$$

Substituting in equation (12), we obtain

$$\frac{Q_{nc}}{Q_o} = \frac{(t_{ad}-t_w)_{nc}}{(t_{ad}-t_w)_o}\left(1 - \frac{\frac{P_i T_{ad}}{T_i P_{ad}} L_t - L_x}{L_c}\right) \qquad (17)$$

This model predicts the reduction in heat transfer Q_{nc}/Q_o rather well (see Figures 12, 13, 14 and 15). The error at the point of maximum disagreement between predicted and experimental values is about 23 percent when applied to the test data taken during this project, and usually much less than that, suggesting that this model is a close representation of the actual behavior of the non-condensable gas inside the heat pipe. However, the limitations of the measuring and recording equipment, the rough estimation of L_x, and the assumption of $T_{nc} = T_{ad}$, may account for the difference between analytical and empirical values of Q_{nc}/Q_o.

Upon examination of the results for the slug model, it is seen that this model predicts heat transfer rates higher than the experimental values for gas loading pressures of 0.446 in. of Hg and 0.843 in. of Hg, but lower heat transfer rates for gas loading pressures of 1.522 in. of Hg and 2.000 in. of Hg. A model that will closely approximate the experimental data is obtained if the interface between vapor and gas is not assumed to be straight. Instead, the interface is assumed to be a circular parabolloid whose dimensions depend on the initial gas loading pressure. (See Figure 16).

Using the same assumptions as for the straight interface slug,

$$Q_o = U(2\pi r_i L_c)(t_{ad}-t_w)_o; \qquad (18)$$

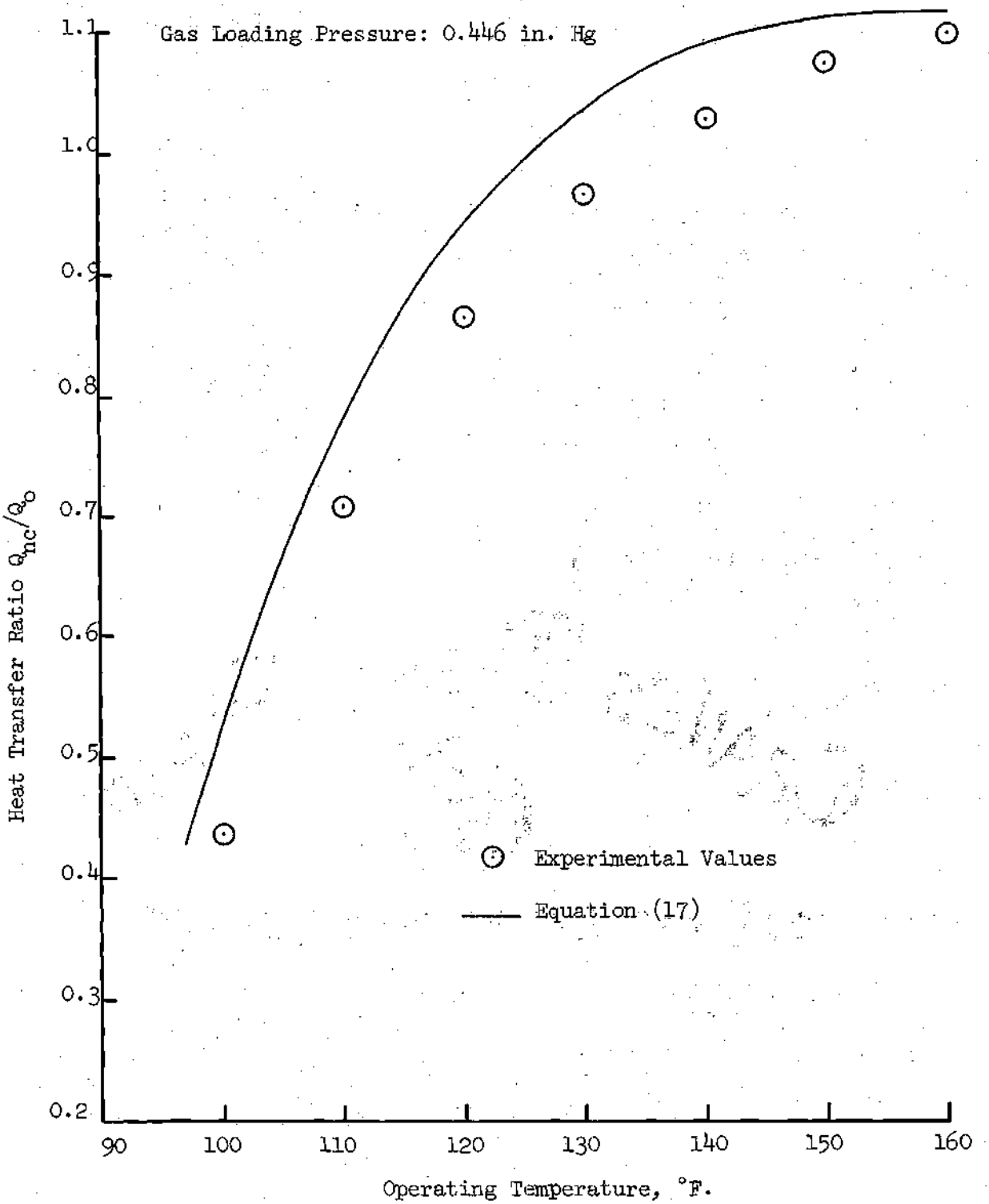

Figure 12. Heat Transfer Ratio Q_{nc}/Q_o Predicted by Slug Model vs. Operating Temperature.

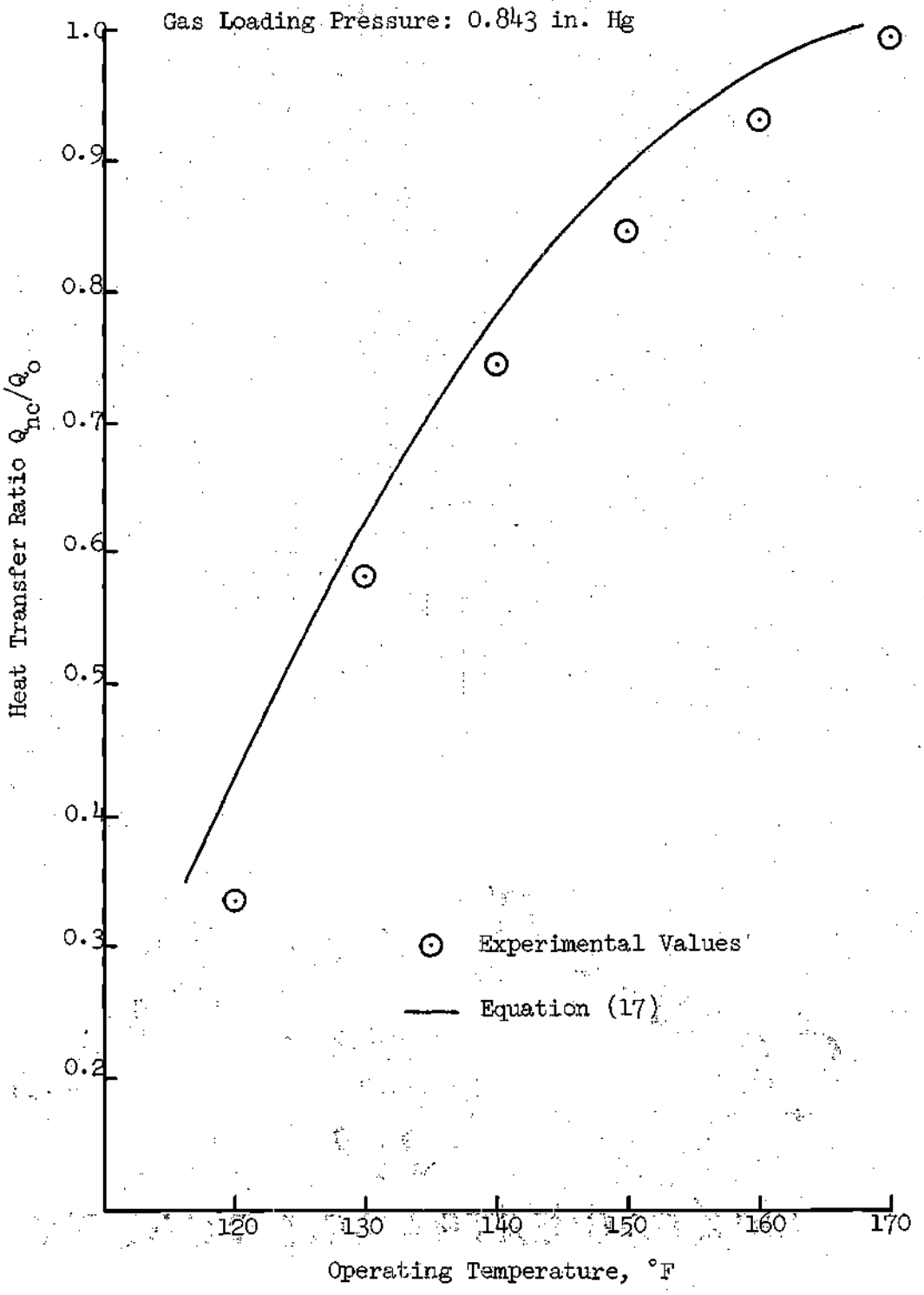

Figure 13. Heat Transfer Ratio Q_{nc}/Q_o Predicted by Slug Model vs. Operating Temperature.

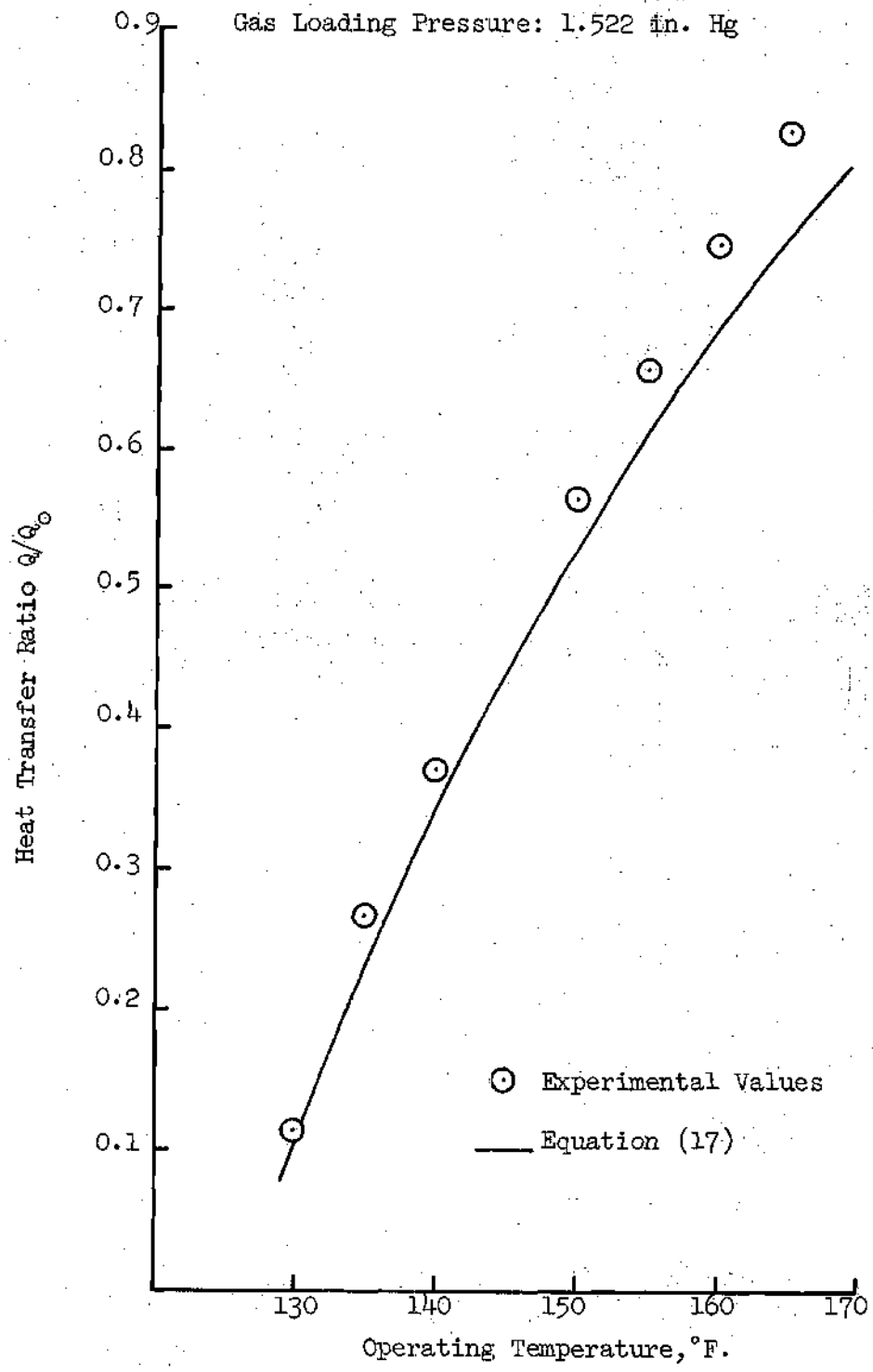

Figure 14. Heat Transfer Ratio Q_{nc}/Q_o Predicted by Slug Model vs. Operating Temperature.

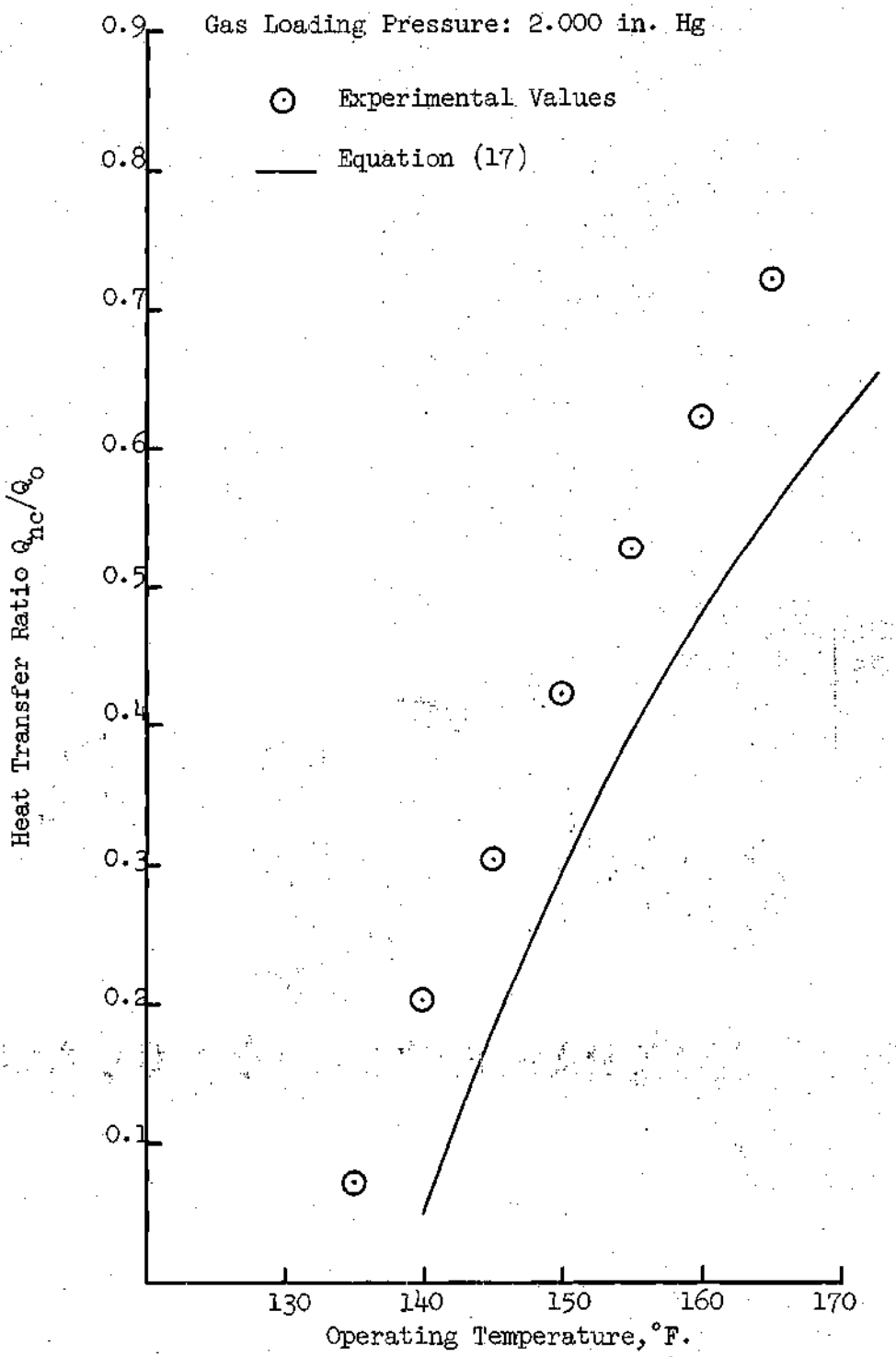

Figure 15. Heat Transfer Ratio Q_{nc}/Q_o Predicted by Slug Model vs. Operating Temperature.

$$Q_{nc} = U(2\pi r_i L_v)(t_{ad}-t_w)_{nc} \tag{19}$$

and,

$$L_v = L_c - (L_{nc} - L_x + L_m) = L_c + L_x - (L_{nc} + L_m) \tag{20}$$

where $L_m = f(m, r_i)$; m being a function of the initial gas loading pressure.

Following a similar procedure to the one for the straight interface model, it is found that

$$V_{nc} = \frac{P_i T_{ad}}{T_i P_{ad}} (\pi r_i^2 L_t)$$

But from Figure (16) it can be seen that

$$V_{nc} = (L_{nc} + L_m)(\pi r_i^2) - V_m$$

where V_m is the volume of the concave or convex section. Thus,

$$(L_{nc} + L_m) = \frac{P_i T_{ad}}{T_i P_{ad}} L_t + \frac{V_m}{\pi r_i^2}$$

and from equation (20)

$$L_v = L_c \left(1 - \frac{\frac{P_i T_{ad}}{T_i P_{ad}} L_t + \frac{V_m}{\pi r_i^2} - L_x}{L_c}\right) \tag{21}$$

Therefore, combining equations (18), (19) and (21)

$$\frac{Q_{nc}}{Q_o} = \frac{(t_{ad}-t_w)_{nc}}{(t_{ad}-t_w)_o} \left(1 - \frac{\frac{P_i T_{ad}}{T_i P_{ad}} L_t + \frac{V_m}{\pi r_i^2} - L_x}{L_c}\right) \tag{22}$$

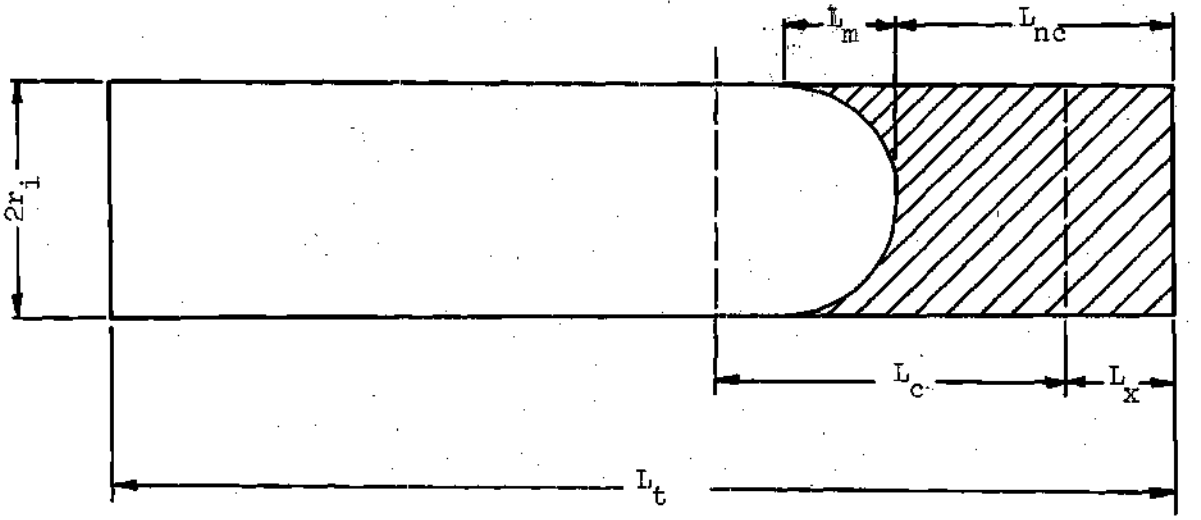

(a) Gas Loading Pressures 0.446 and 0.893 in. Hg

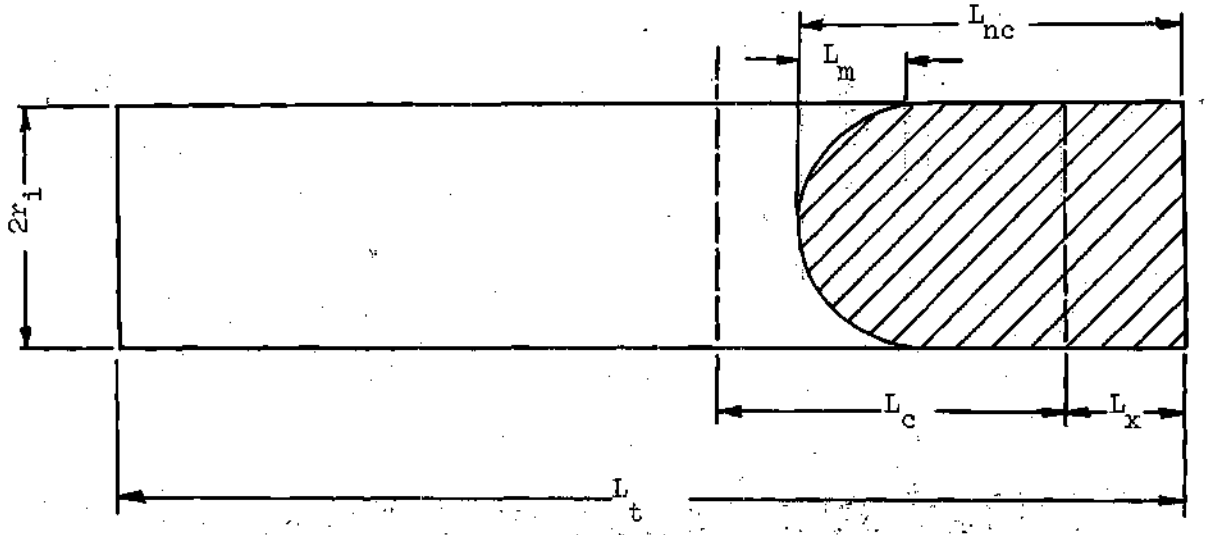

(b) Gas Loading Pressures 1.522 and 2.000 in. Hg

Figure 16. Modified Slug Model

V_m is found as follows, (see Figure (17):

$$g(r) = f_{(m)}r^2$$

$$V_m = \int_o^{g(r_i)} 2\pi r\left(\frac{r}{2}dg\right) = \int_o^{g(r_i)} \pi r^2 dg = \int_o^{g(r_i)} \frac{\pi g(r)}{f_{(m)}}\, dg$$

$$V_m = \frac{\pi}{2f_{(m)}} - [g(r_i)]^2 = \frac{\pi}{2f_{(m)}}[f_{(m)}r_i^2]^2$$

$$\frac{V_m}{\pi r_i^2} = \frac{f_{(m)}}{2} r_i^2 \qquad (23)$$

Define $m = \frac{100\ P_i}{P_t}$ and find f(m) using a Lagrange interpolation. Let

$$f_{(m)} = am^3 + bm^2 + cm + d \qquad (24)$$

The coefficients a, b, c, and d are found by fitting the predicted heat transfer rate to the experimental results using test No. 9 as the reference Q_o, and they are:

a = - 0.1414

b = + 1.0374

c = - 6.1810

d = + 16.474

The reduction in heat transfer as predicted by this model is shown in Figures 18, 19, 20, and 21 which indicate a very close agreement between model and experimental values.

The validity of this empirical correlation can be tested by comparing the predicted and experimental values of Q_{nc}/Q_o obtained when

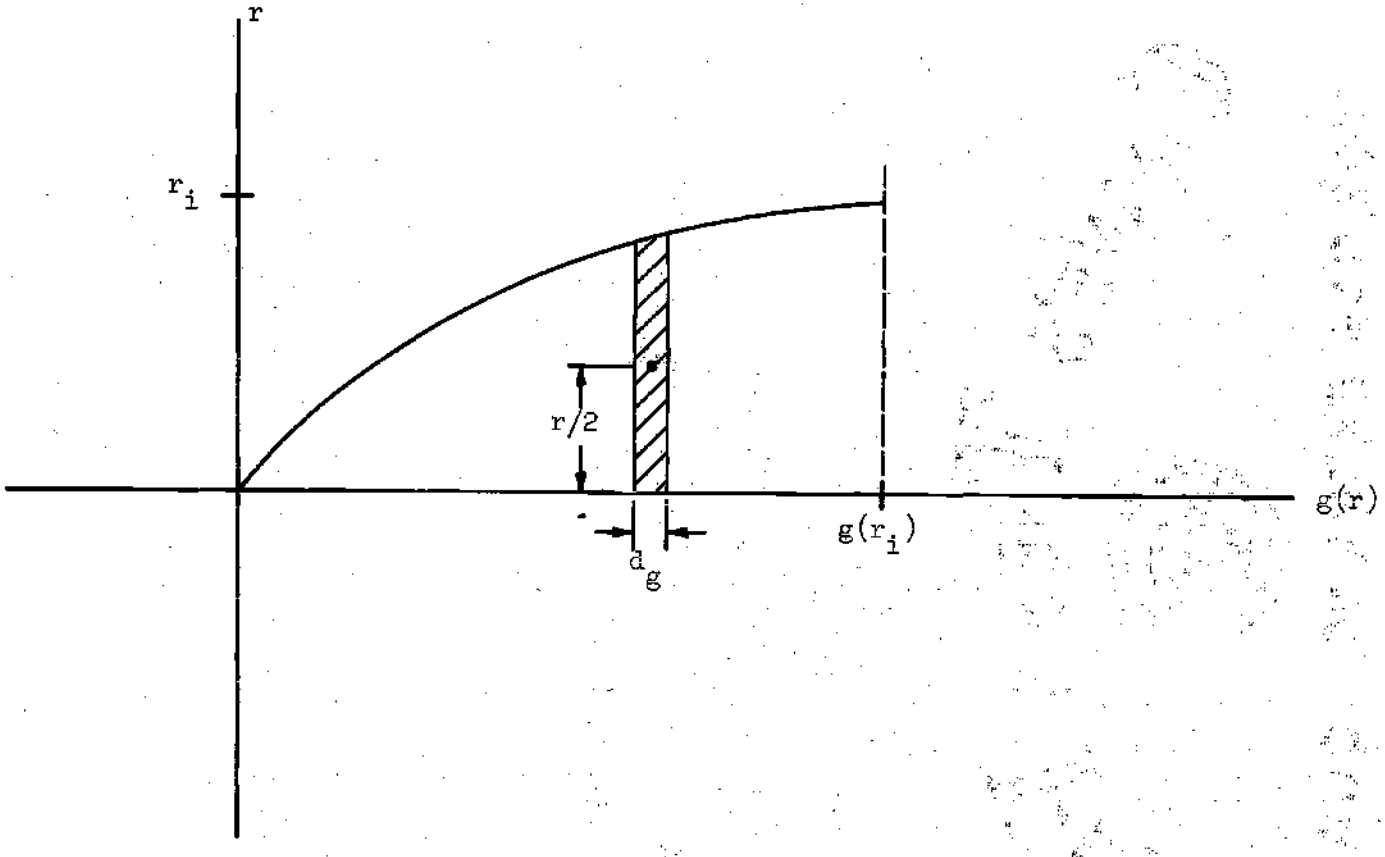

Figure 17. Calculation of V_m

test No. 6 is used as the reference Q_o. Figures 22, 23, 24 and 25 show the results, again, to be in close agreement.

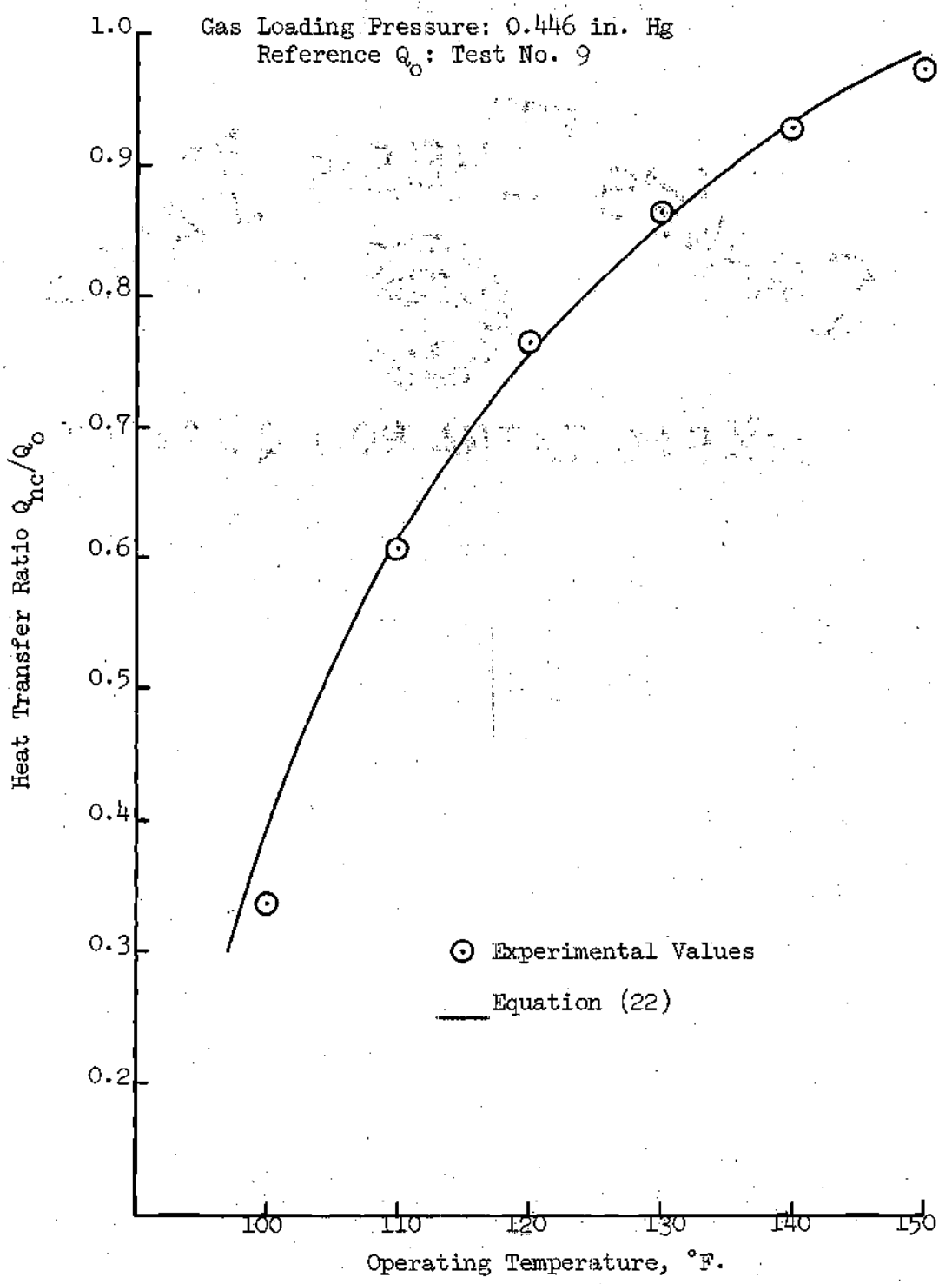

Figure 18. Heat Transfer Ratio Q_{nc}/Q_o Predicted by Modified Slug Model vs. Operating Temperature.

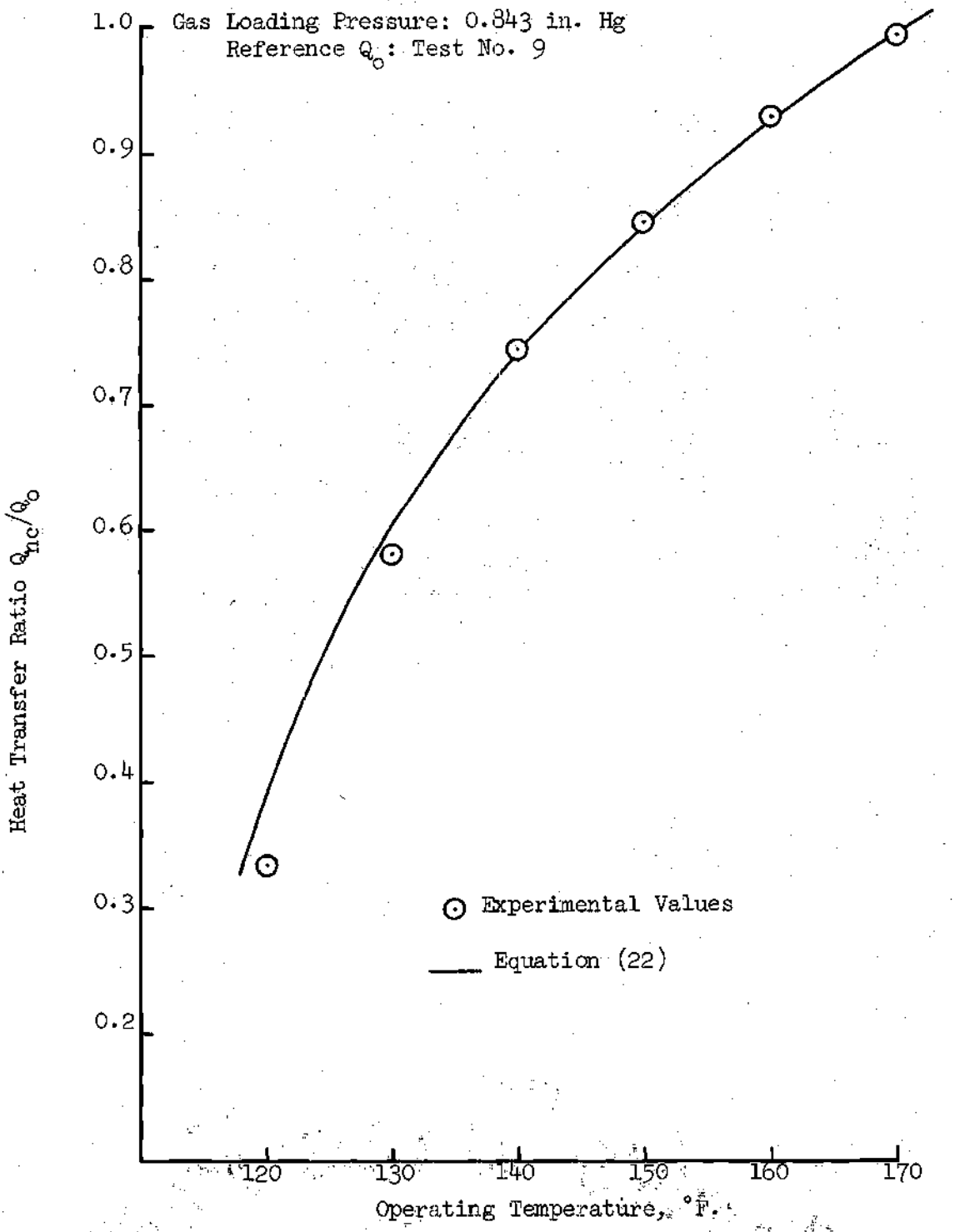

Figure 19. Heat Transfer Ratio Q_{nc}/Q_o Predicted by Modified Slug Model vs. Operating Temperature.

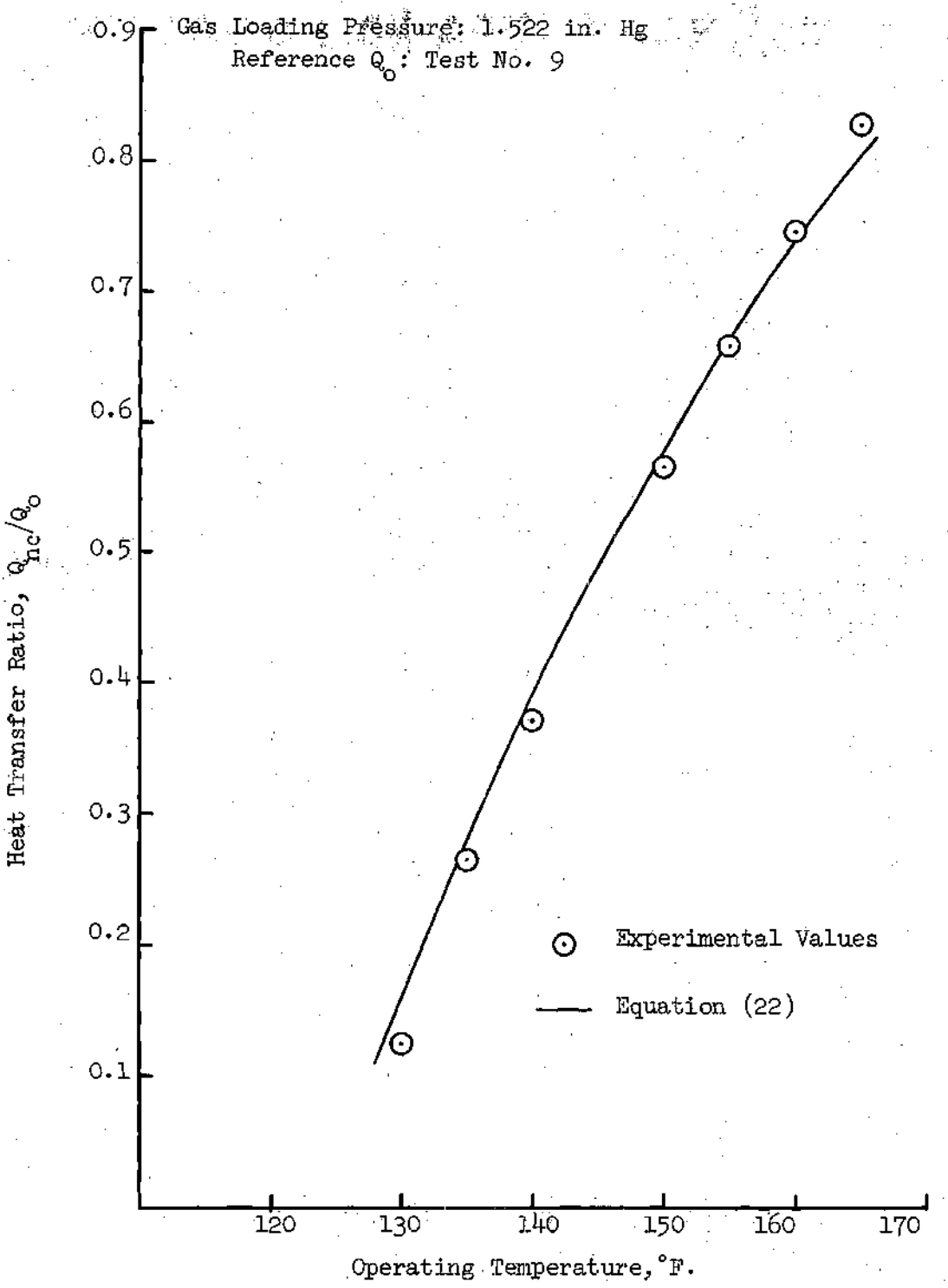

Figure 20. Heat Transfer Ratio Q_{nc}/Q_o Predicted by Modified Slug Model vs. Operating Temperature.

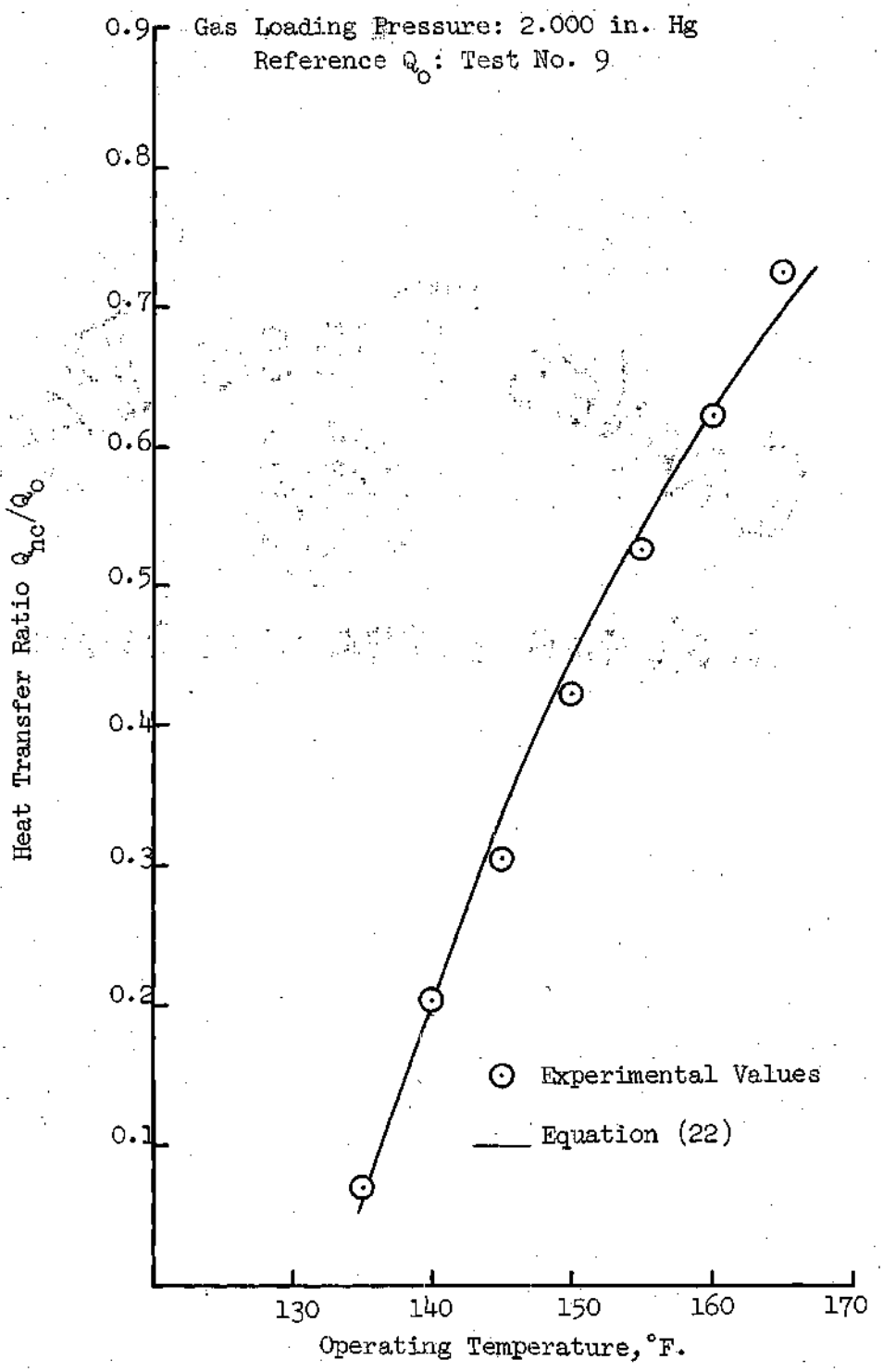

Figure 21. Heat Transfer Ratio Q_{nc}/Q_o Predicted by Modified Slug Model vs. Operating Temperature.

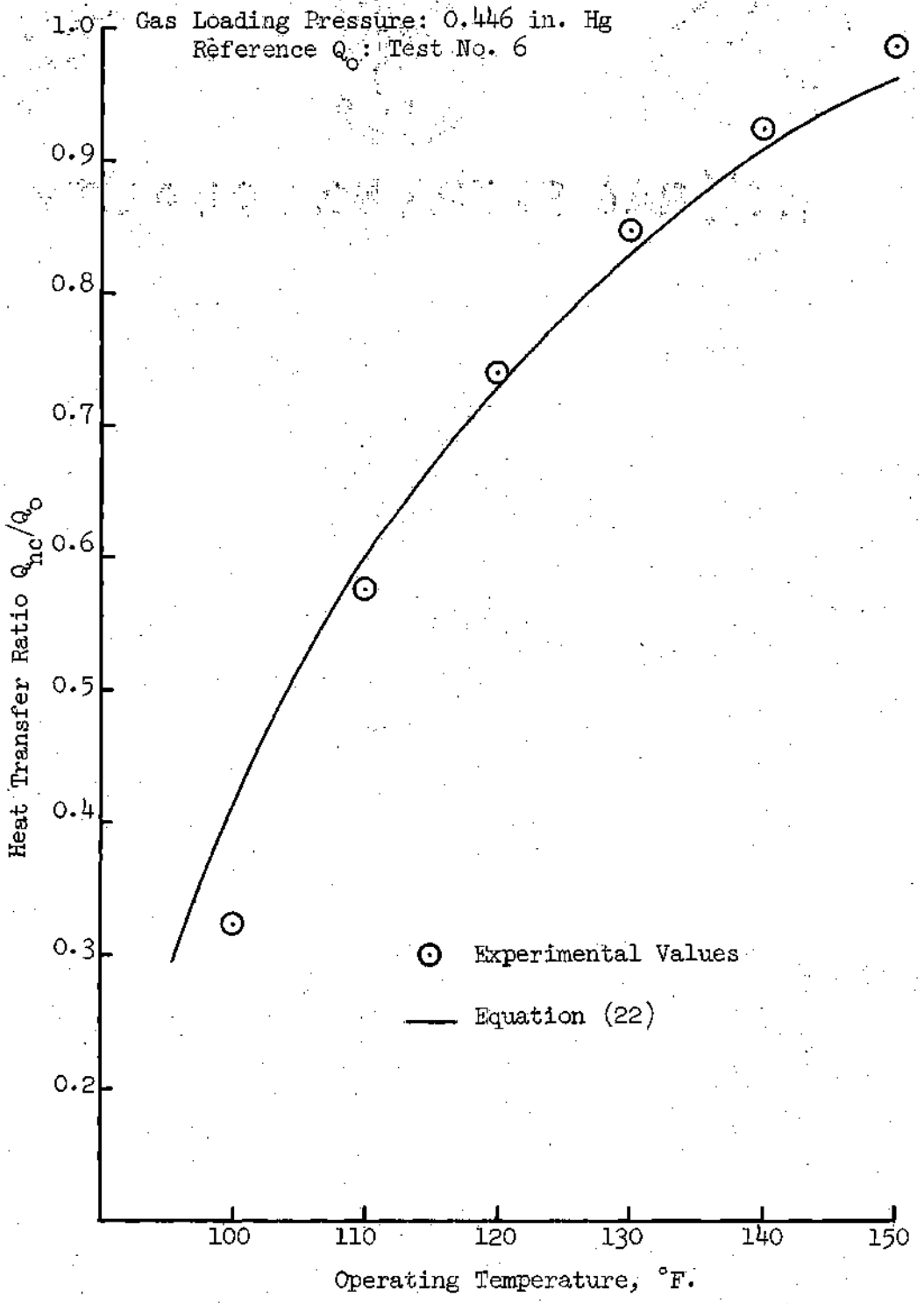

Figure 22. Heat Transfer Ratio Q_{nc}/Q_o Predicted by Modified Slug Model vs. Operating Temperature.

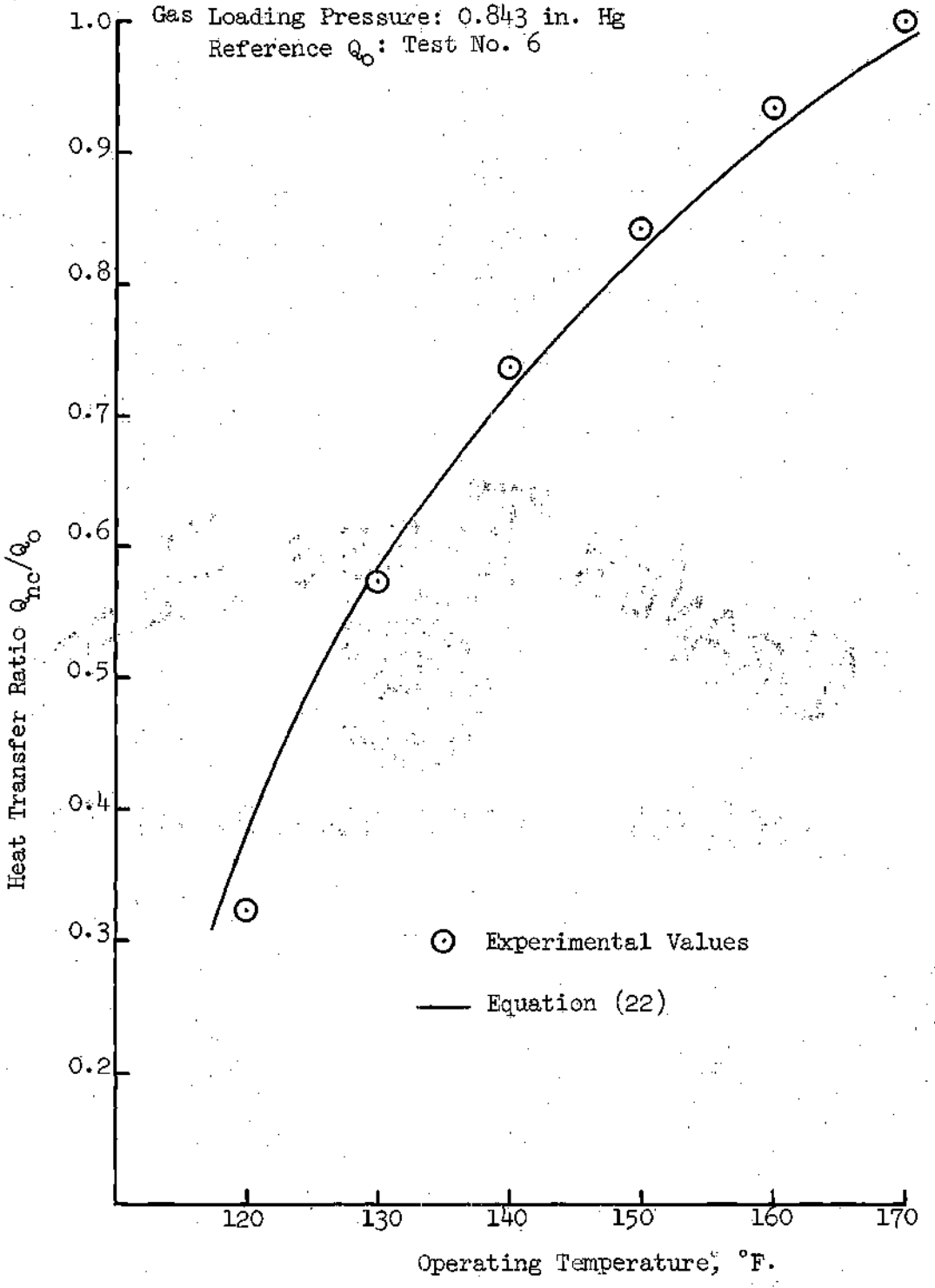

Figure 23. Heat Transfer Ratio Q_{nc}/Q_o Predicted by Modified Slug Model vs. Operating Temperature.

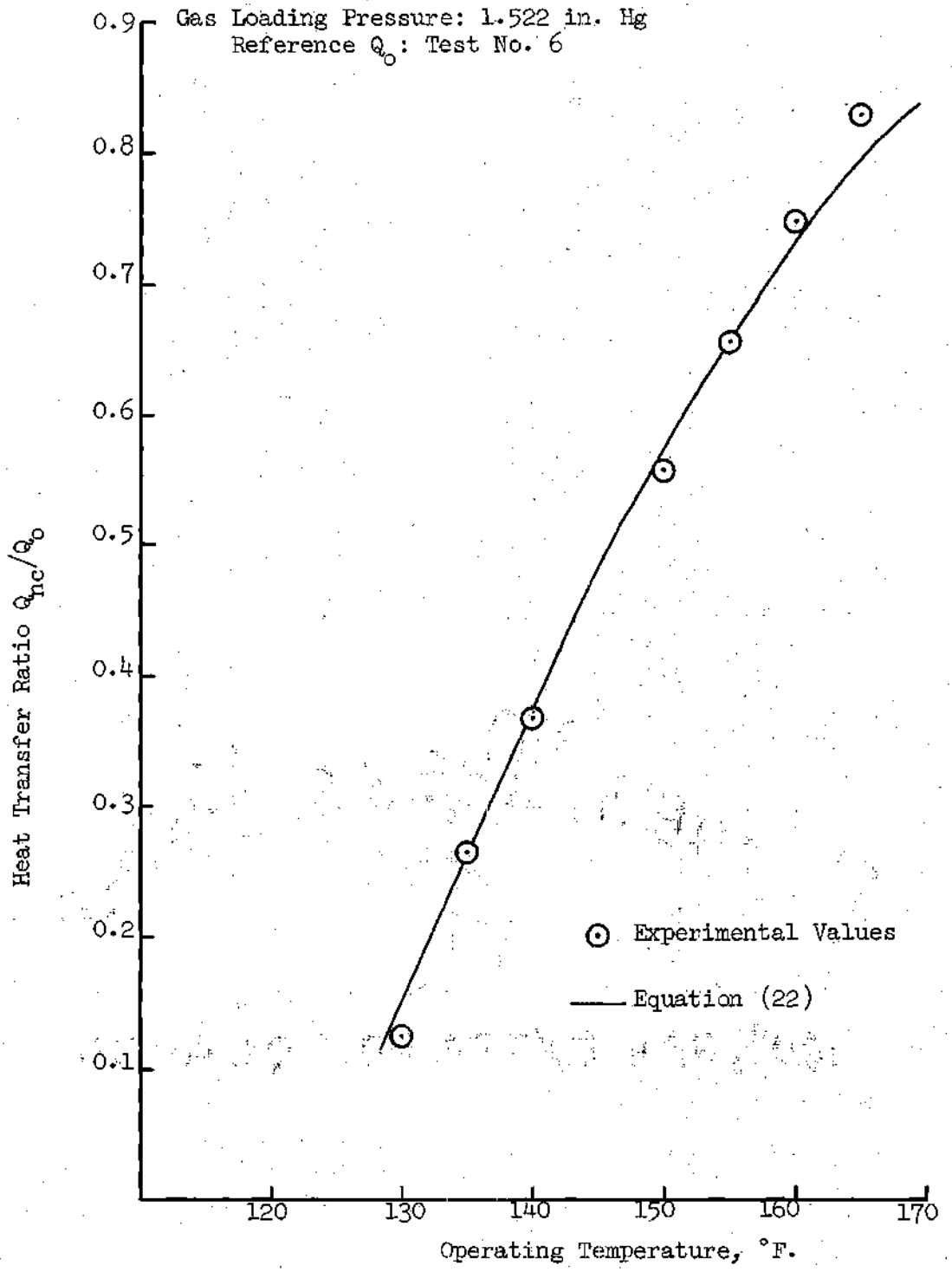

Figure 24. Heat Transfer Ratio Q_{nc}/Q_o Predicted by Modified Slug Model vs. Operating Temperature.

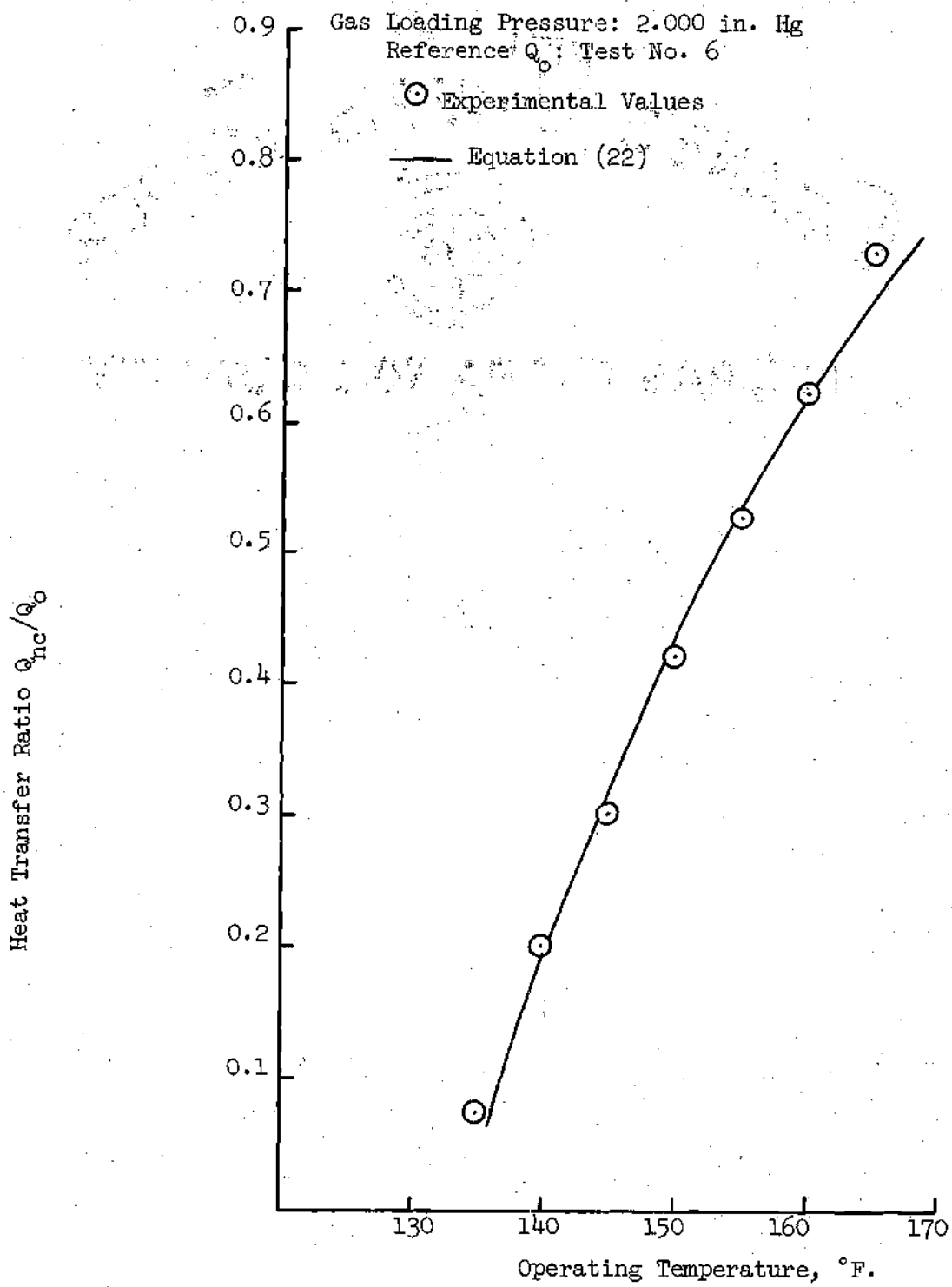

Figure 25. Heat Transfer Ratio Q_{nc}/Q_o Predicted by Modified Slug Model vs. Operating Temperature.

CHAPTER V

DIMENSIONAL ANALYSIS

The performance of a heat pipe loaded with a non-condensable gas can be better studied if the parameters governing heat pipe behavior can be grouped into non-dimensional quantities. Graphs relating these non-dimensional quantities can then be made, and generalized performance charts, possibly, obtained.

The following are considered to be the governing parameters in the performance of the gas-loaded heat pipe:

$$Q,\ \sigma,\ \rho_v,\ \rho_l,\ \mu_v,\ \mu_l,\ h_{fg},\ r_i,\ L_t,\ L_c,\ \frac{P_i}{P_{st}},\ \frac{T_i}{T_{st}},\ T_{ad},\ T_{ad} - T_w.$$

Using the Buckingham π-theorem, various non-dimensional quantities can be obtained. These are then grouped together to form the following non-dimensional groups:

$$\frac{Q}{\sigma r_i (h_{fg})^{\frac{1}{2}}},\ \frac{Q\sigma(\rho_l\rho_\sigma)^{\frac{1}{2}}}{h_{fg}(\mu_l\mu_v)^{\frac{1}{2}}},\ \frac{P_i T_{st} L_t}{T_i P_{st} L_c},\ \frac{T_{ad}-T_w}{T_{ad}}$$

These groups can be re-written as products, and physical significance can be attached to some of the factors.

For instance, recalling that

$$Q = \dot{m}h_{fg} = (\rho_v V_v A_i)h_{fg} = (\rho_l V_l A_l)h_{fg}$$

and that

$$A_i = \pi d_i^2/4$$

The dimensionless group $Q/\sigma r_i (h_{fg})^{\frac{1}{2}}$ can be written as

$$\frac{4\pi(d_i/d_c)\ (\rho_v V_v r_i/\mu_v)\ (\mu_v\sqrt{h_{fg}}/r_i)}{(2\sigma/r_c)}$$

The factor $(d_i d_c)$ is the ratio of the diameter of the vapor space to the mean capillary pore diameter.

The term $(\rho V_v r_i/\mu_v)$ is the vapor Reynolds number.

The term $2\sigma/r_c$ is related to the capillary pumping capacity of the wick-liquid structure.

At the present time no physical significance can be attached to the term $\mu_v\sqrt{h_{fg}}/r_i$.

Similarly, the group $\frac{Q\sigma(\rho_l\rho_v)^{\frac{1}{2}}}{h_{fg}(\mu_l\mu_v)^{\frac{3}{2}}}$ can be written as

$$(\frac{\rho_v V_v r_i}{\mu_v})^{\frac{1}{2}}\ (\frac{\rho_l V_l A_l}{\mu_l})^{\frac{1}{2}}\ (\sigma/\mu_l)\ (\frac{\pi r_i \rho_l \rho_v}{\mu_l^4 \mu_v^6})^{\frac{1}{2}}$$

Where the term $(\frac{\rho_v V_v r_i}{\mu_v})^{\frac{1}{2}}$ is the vapor Reynolds number to the one-half power and term $(\frac{\rho_l V_l A_l}{\mu_l})^{\frac{1}{2}}$ can be taken as the liquid Reynolds number to the one-half power.

Also, $\frac{\sigma}{\mu_l}$ can be taken as the ratio of the surface tension forces to the viscous forces in the liquid.

No physical significance can be attached at present to the term

$$(\frac{\pi r_i \rho_l \rho_v}{\mu_l^4 \mu_v^6})^{\frac{1}{2}}$$

The dimensionless group $(P_i T_{st} L_t / T_i P_{st} L_c)$ can be written as

$$\left(\frac{m_A R_{nc} T_{st}/P_{st}}{m_A R_{nc} T_i/P_i}\right)\left(\frac{2\pi r_i L_t}{2\pi r_i L_c}\right)$$

where the first factor is the ratio of the volume that the injected gas would fill at standard pressure and temperature to the inner volume of the heat pipe. The second factor is the ratio of the area of the vapor-liquid interface to the area of the condenser.

Finally the dimensionless number $\frac{T_{ad}-T_w}{T_{ad}}$ is the ratio of the temperature difference which causes the condenser heat transfer to the operating temperature of the heat pipe.

It is desirable that the non-dimensional quantitites take a form such that, given an operating condition, the rate of heat transfer can be obtained once the geometry of the pipe and the working fluid have been selected. The following relationships are selected:

$$\frac{Q}{\sigma r_i \sqrt{h_{fg}}} = f_1\left(\frac{P_i T_{st} L_t}{T_i P_{st} L_c}, \frac{T_{ad}-T_w}{T_{ad}}\right), \text{ and}$$

$$\frac{Q\sigma(\rho_l \rho_v)^{\frac{1}{2}}}{h_{fg}(\mu_l \mu_v)^{\frac{3}{2}}} = f_2\left(\frac{P_i T_{st} L_t}{T_i P_{st} L_c}, \frac{T_{ad}-T_w}{T_{ad}}\right)$$

The first relationship is for a heat pipe using water as the working fluid. The second is intended to be general such that it can be applied regardless of the working fluid used.

For simplicity and brevity the following nomenclature is used. Let

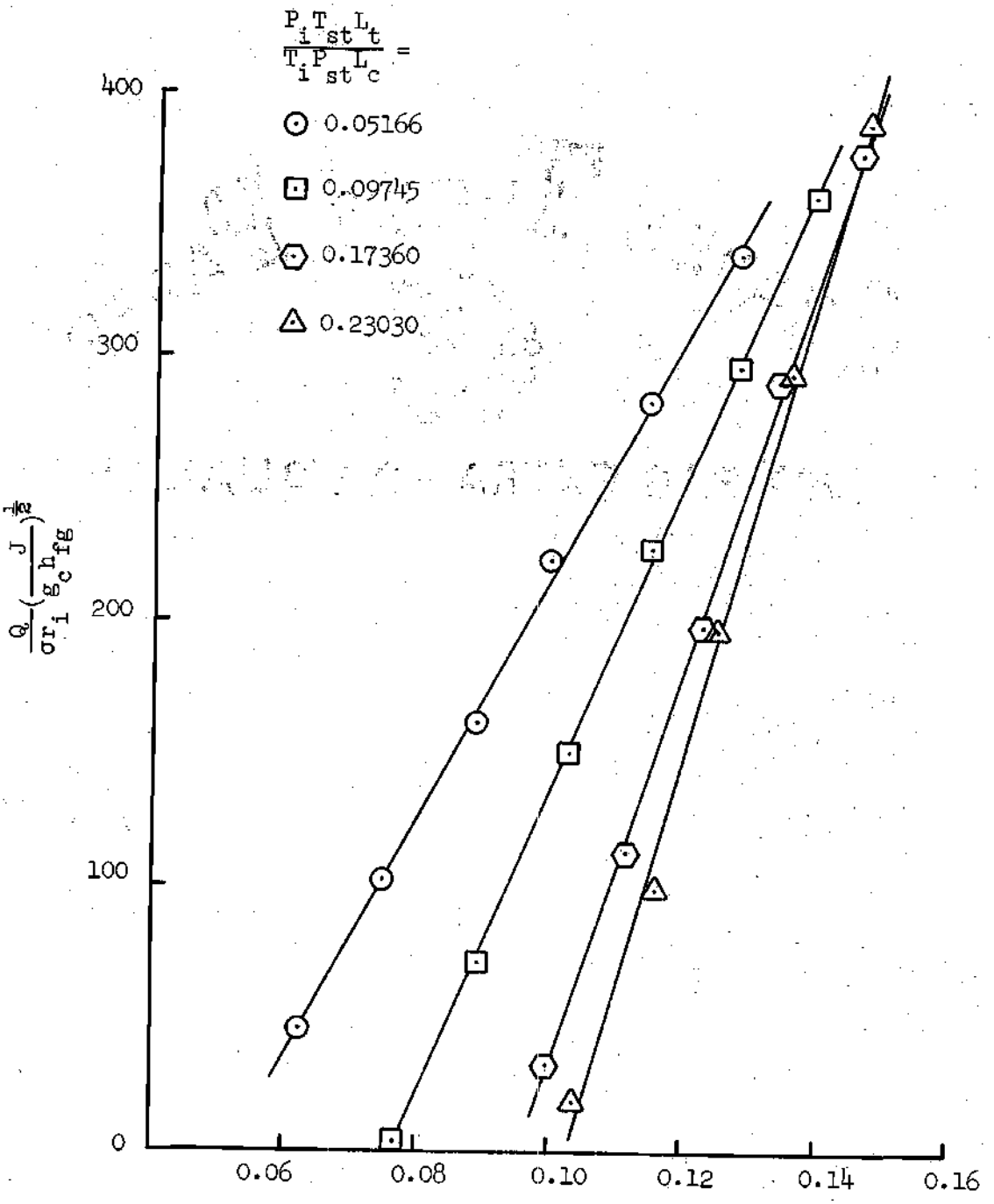

Figure 26. $\frac{Q}{\sigma r_i}\left(\frac{J}{g_c h_{fg}}\right)^{\frac{1}{2}}$ vs. $\frac{T_{ad}-T_w}{T_{ad}}$.

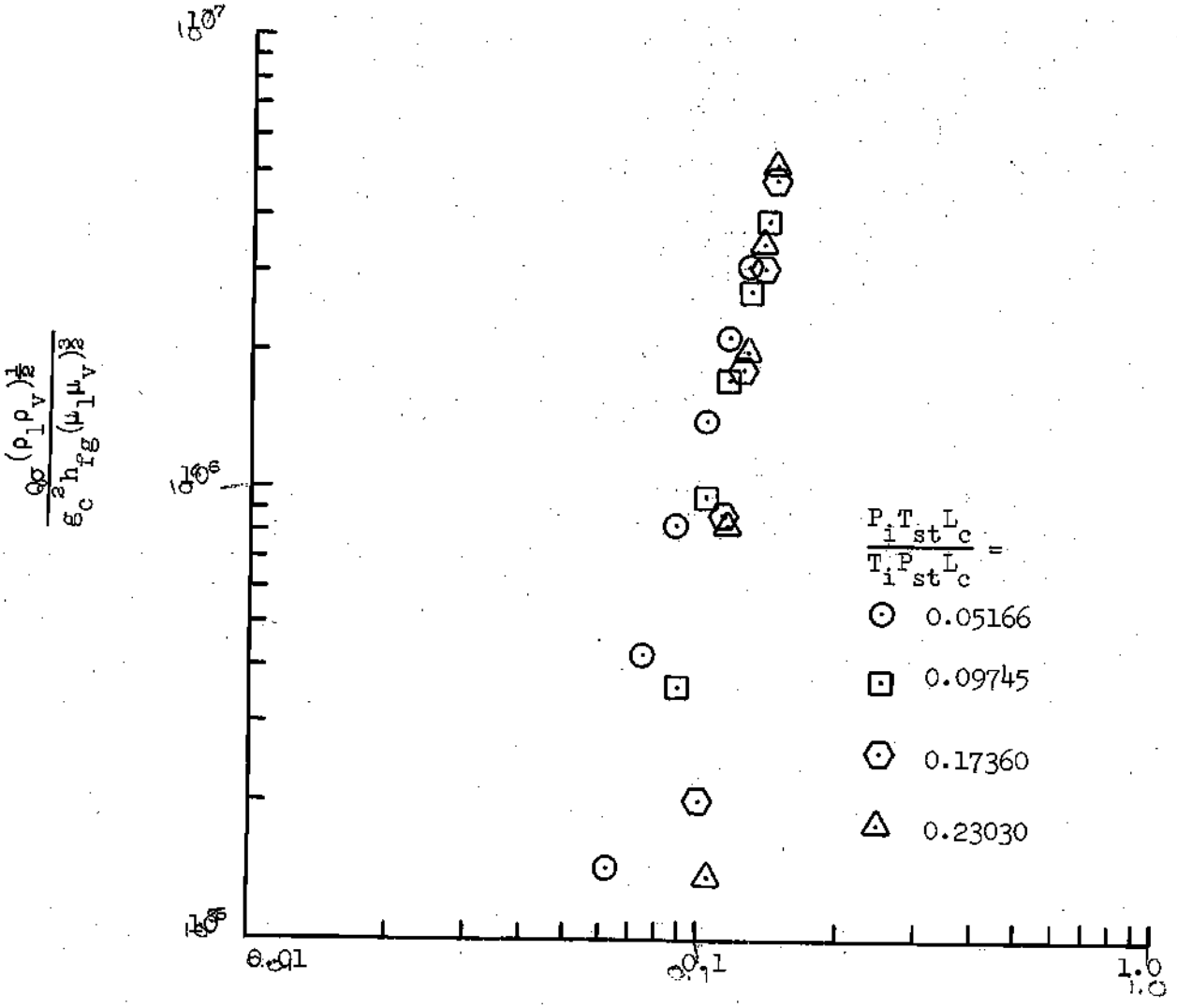

Figure 27. $\frac{Q_\sigma(\rho_l\rho_v)^{\frac{1}{2}}}{g_c^{\frac{2}{3}}h_{fg}(\mu_l\mu_v)^{\frac{1}{3}}}$ vs. $\frac{T_{ad}-T_w}{T_{ad}}$.

$$Q_1^* = \frac{Q}{\sigma r_i \sqrt{h_{fg}}}, \quad Q_2^* = \frac{Q\sigma(\rho_l \rho_v)^{\frac{1}{2}}}{h_{fg}(\mu_l \mu_v)^{\frac{3}{2}}},$$

$$P_i^* = \frac{P_i T_{st} L_t}{T_i P_{st} L_c}, \text{ and } T_{ad}^* = \frac{T_{ad} - T_w}{T_{ad}}$$

Curves of Q_1^* versus T_{ad}^* for various P_i^* are shown in Figure 26. From these curves, an empirical correlation between Q_1^*, T_{ad}^* and P_i^* can be obtained. The relationship

$$Q_1^* = (3215 + 25{,}250\ P_i^*)(T_{ad}^*) - (50 + 3900\ P_i^*) \qquad (25)$$

seems to describe within 10 percent the performance of this particular heat pipe as shown by the comparison between predicted and experimental values in Figures 28, 29, 30, and 31.

A curve of Q_2^* versus T_{ad}^* for various P_i^* is shown in Figure 27. This curve indicates that the influence of the amount of non-condensable gas present inside the heat pipe is more significant at low operating points.

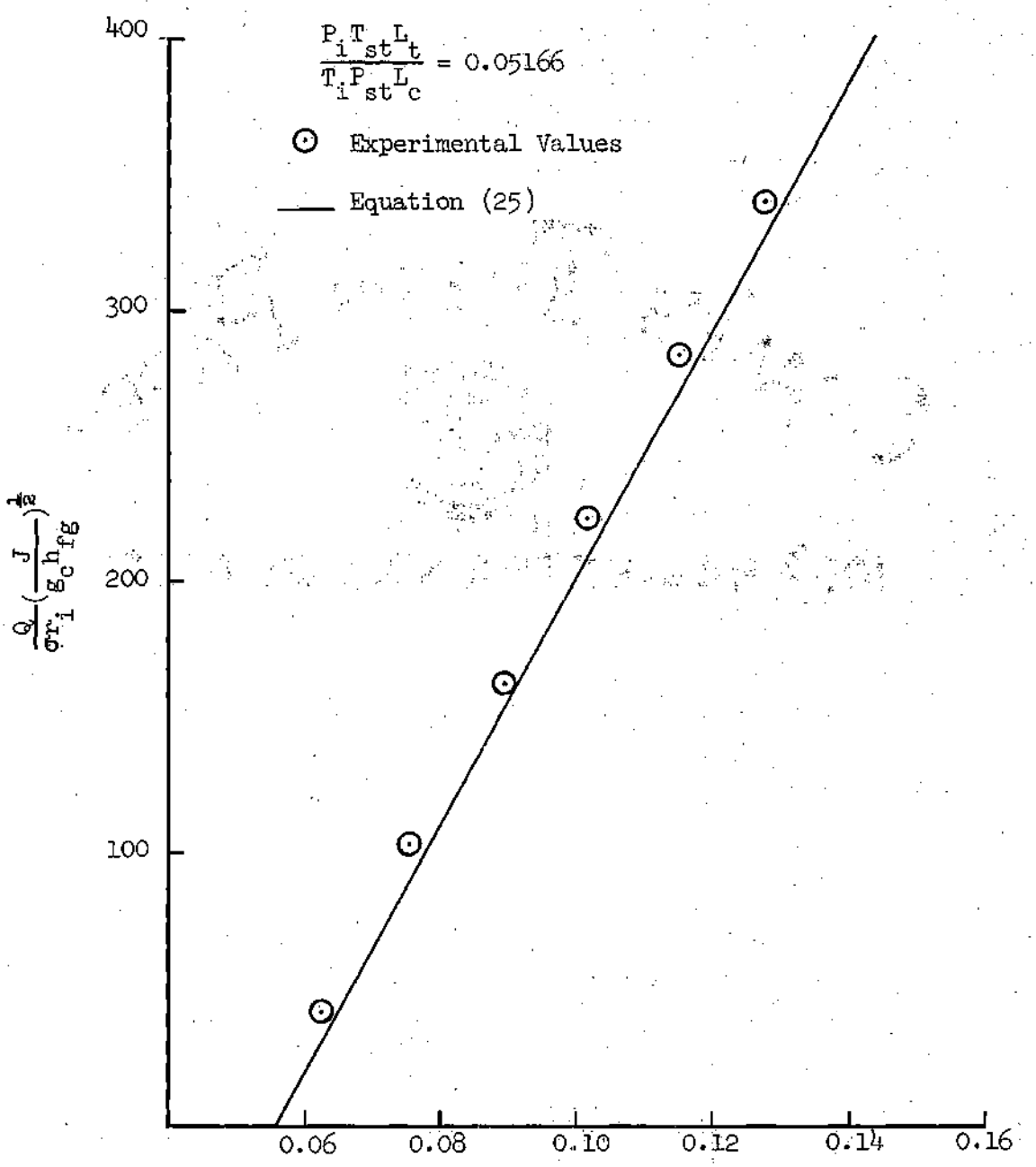

Figure 28. Values of $\frac{Q}{\sigma r_i}\left(\frac{J}{g_c h_{fg}}\right)^{\frac{1}{2}}$ Predicted by Equation (25).

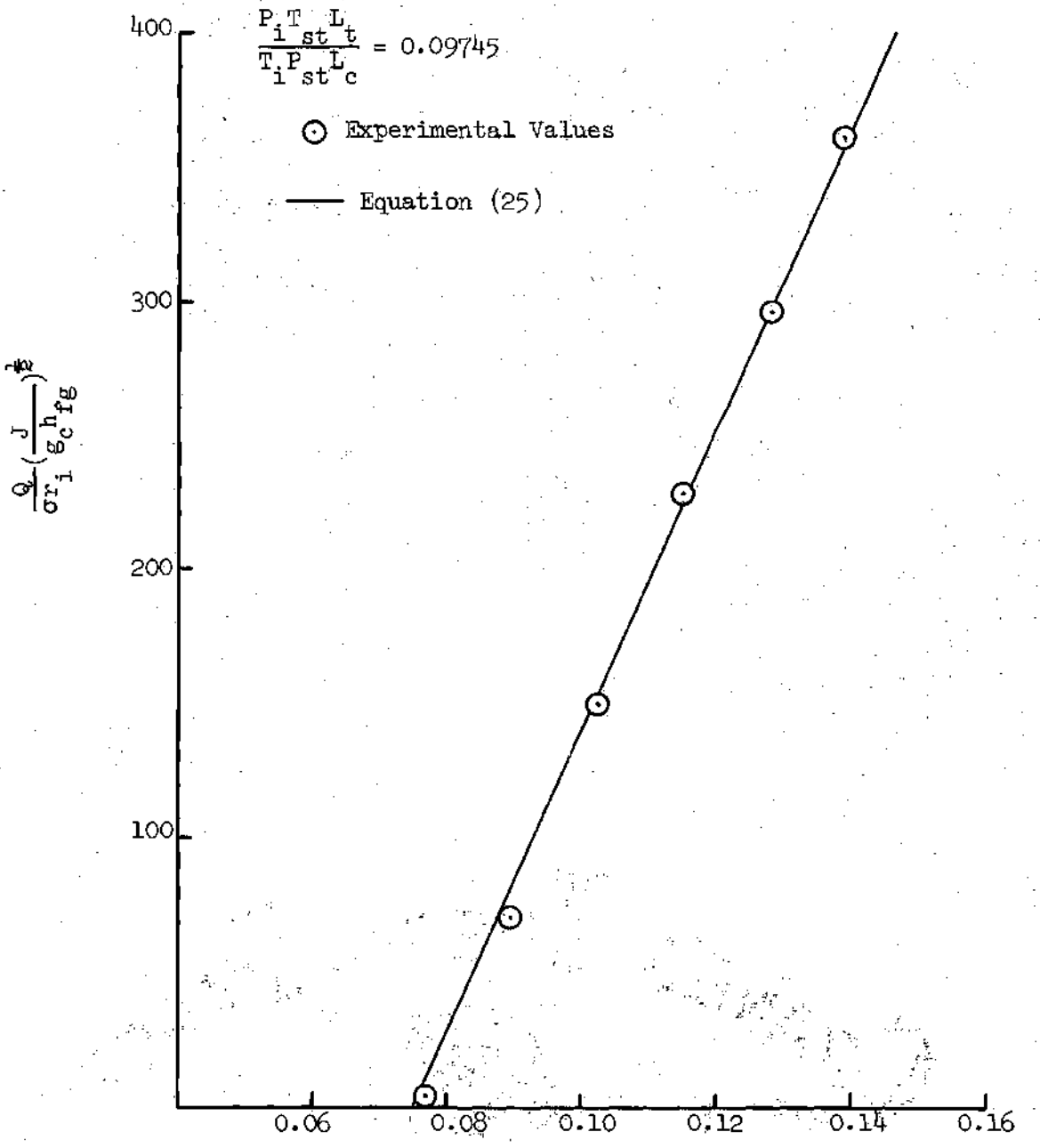

Figure 29. Values of $\frac{Q}{\sigma r_i}\left(\frac{J}{g_c h_{fg}}\right)^{\frac{1}{2}}$ as Predicted by Equation (25).

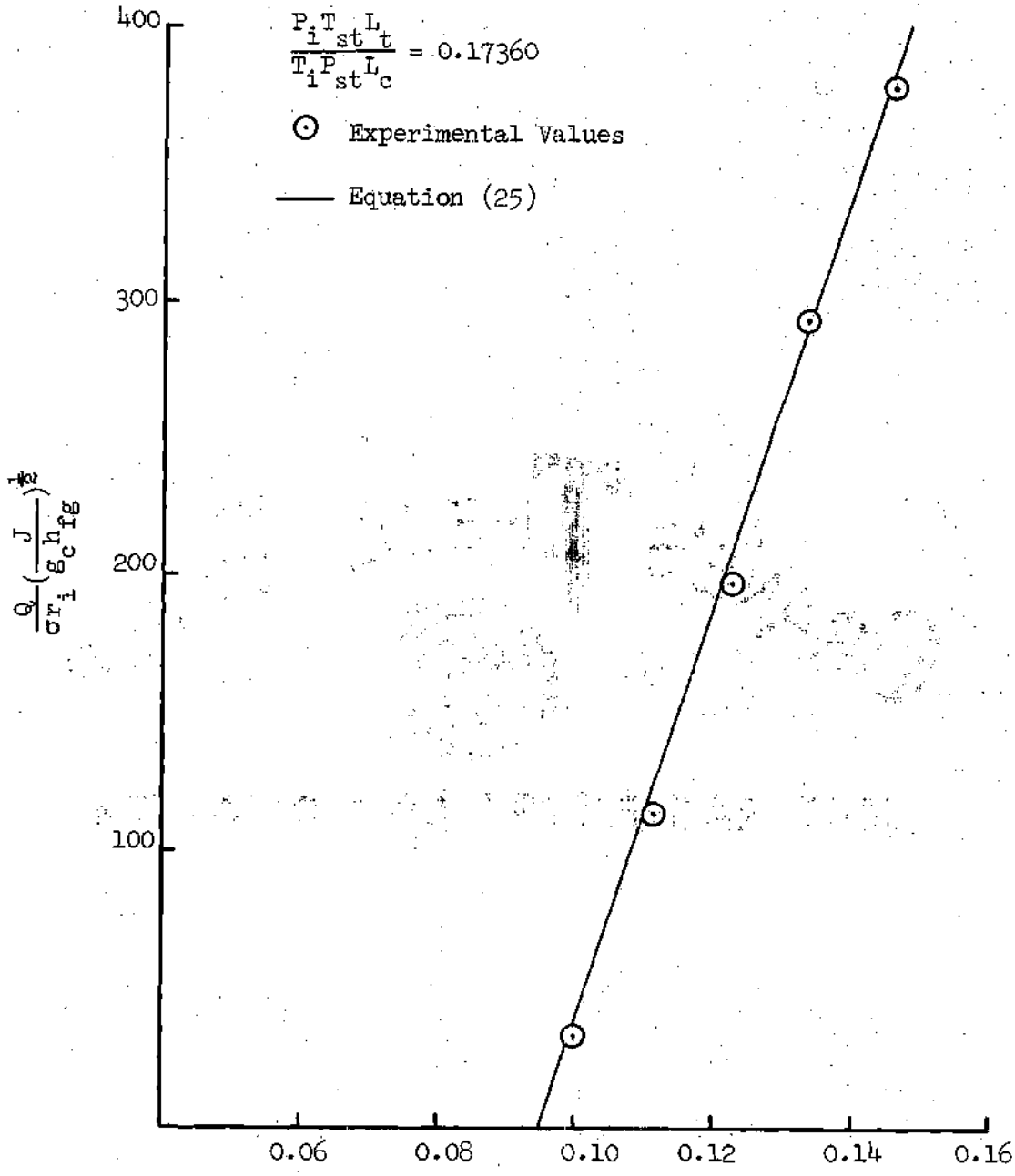

Figure 30. Values of $\frac{Q}{\sigma r_i}(\frac{J}{g_c h_{fg}})^{\frac{1}{2}}$ Predicted by Equation (25)

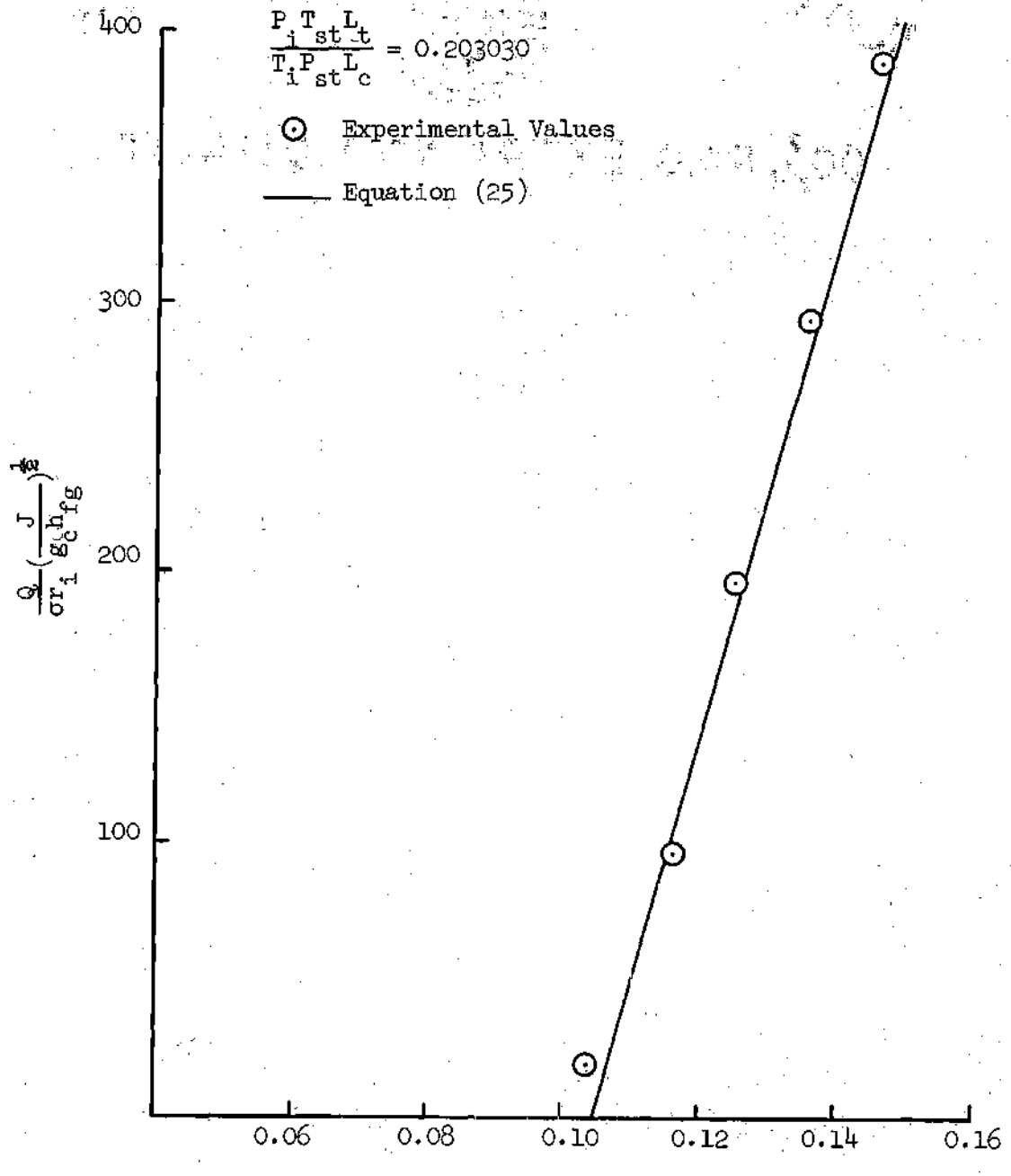

Figure 31. Values of $\frac{Q}{\sigma r_i}\left(\frac{J}{g_c h_{fg}}\right)^{\frac{1}{2}}$ as Predicted by Equation (25).

CHAPTER VI

SIMPLIFIED THEORY OF NON-CONDENSABLE GAS MOVEMENT

A better understanding of the influence of non-condensable gases on the performance of heat pipes can be developed if the movement of the gas inside the heat pipe can be studied and its distribution in the vapor space, as a function of the operating variables, can be obtained.

Certain simplifying assumptions are necessary in the development of the theory that follows. It is postulated that the heat pipe operates with small pressure and temperature gradients in the vapor space (6) (8); heat losses are considered negligible in magnitude compared to the heat transfered; the injection velocity and the rejection velocity are assumed uniform along the evaporator and the condenser, respectively (9); the total density is assumed to remain constant; it is also assumed that the non-condensable gas moves with the same convective velocity as the vapor; finally, it is postulated that the velocity profile is uniform over any cross section of the vapor space (9) and the same goes for the concentration profile.

When the non-condensable gas is injected into the pipe (before the working fluid injection), it is distributed uniformly inside the heat pipe. As the heat pipe is loaded with the working fluid and put into operation, the flow of vapor from evaporator to condenser carries the non-condensable gas to the condenser end, thus creating a concentration gradient of non-condensable gas.

To study the possibility of back-diffusion of the gas, assume a model as shown in Figure 32 where a vapor-gas mixture is moving with a constant convective velocity V_x, and let the concentration of gas be zero at one end, and one at the opposite end, such that the diffusive flow opposes the convective flow. For the element shown,

$$(\rho W_A V_x) + (-\rho D\frac{dW_A}{dx}) = (\rho W_A V_x) + \frac{d}{dx}(\rho W_A V_x)dx + (-\rho D\frac{dW_A}{dx}) + \frac{d}{dx}(-\rho D\frac{dW_A}{dx})dx$$

After some manipulation, the following differential equation is obtained:

$$\frac{d^2 W_A}{dx^2} - \frac{V_x}{D}\frac{dW_A}{dx} = 0 \qquad (26)$$

The boundary conditions are:

$W_A(0) = 0$

$W_A(L_t) = 1.$

The solution of this equation is

$$W_A(x) = \frac{1 - \exp(\frac{V_x}{D} x)}{1 - \exp(\frac{V_x}{D} L_t)} \qquad (27)$$

Using the experimental data, numbers can be substituted in this expression. For a typical operating point, say P_i = 1.522 in. of Hg, t_{ad} = 150°F, (36)

$$D = \frac{T^{2.334}}{P_t} \times (4.07157 \times 10^{-7}) \text{ cm}^2/\text{sec} \qquad (28)$$

where T and P_t represent the total temperature and pressure, respectively.

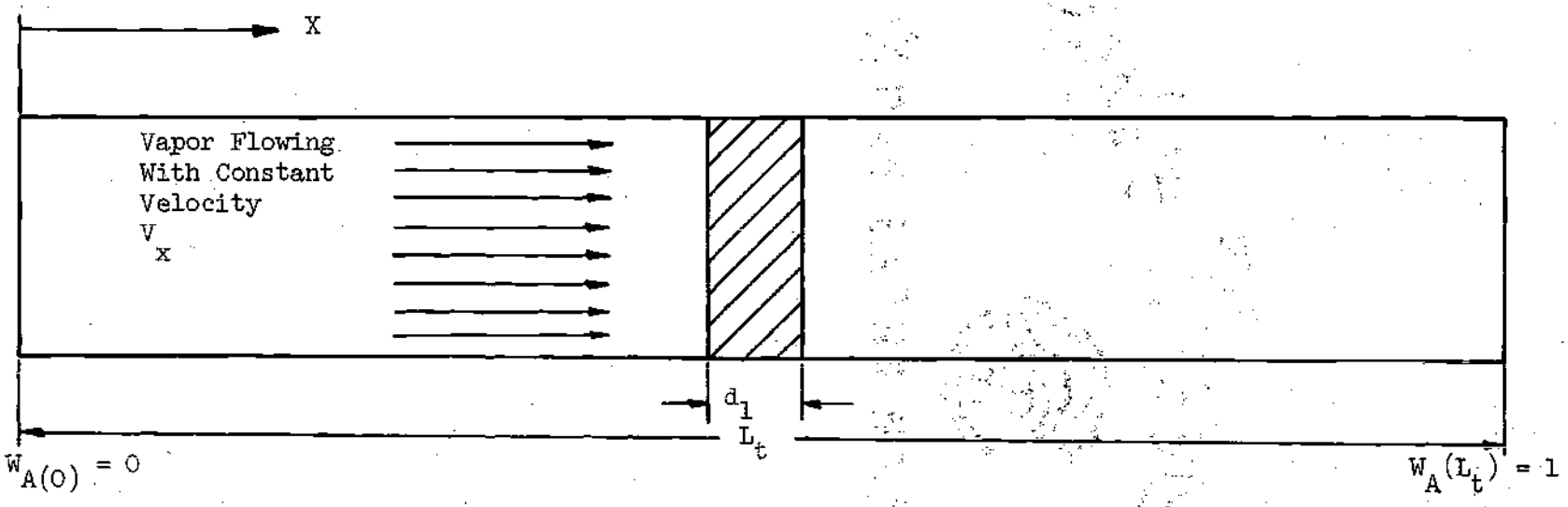

Figure 32. Constant Velocity Model

$$D = 1.161446 \text{ cm}^2/\text{sec} = 1.25 \times 10^{-3} \text{ ft}^2/\text{sec}$$

and

$$L_t = 1.5 \text{ ft, from the pipe dimensions.}$$

Suppose, for instance, that it is desired to know what the value of V_x must be so that at $x = 0.50$ ft., W_A take a value of, say, 0.22.

From equation (27),

$$[0.22][1 - \exp(\frac{1.5V_x}{1.25 \times 10^{-3}})] = 1 - \exp(\frac{0.50V_x}{1.25 \times 10^{-3}})$$

By trial and error it is found that $V_x = 10^{-3}$ ft/sec. This value must now be compared with the experimental values for V_x. An approximate value for V_x can be obtained knowing that

$$Q = \dot{m} h_{fg} \text{ and } \dot{m} = \rho_v V_x A_i$$

therefore

$$V_x = \frac{Q}{\rho_v A_i h_{fg}} \tag{29}$$

From the experimental data, it can be calculated that the smallest vapor velocity will be of the order of 1 ft/sec. Therefore it can be concluded that a concentration profile of gas such that $W_A|x = 0.50 \approx 0.22$ will not exist for the model proposed.

Another model, more realistic than the previous one, will give even more insight into the distribution of the non-condensable gas. Consider the arrangement shown in Figure 33, in which a mixture of vapor and gas flows with decreasing velocity towards the end of a pipe where a high

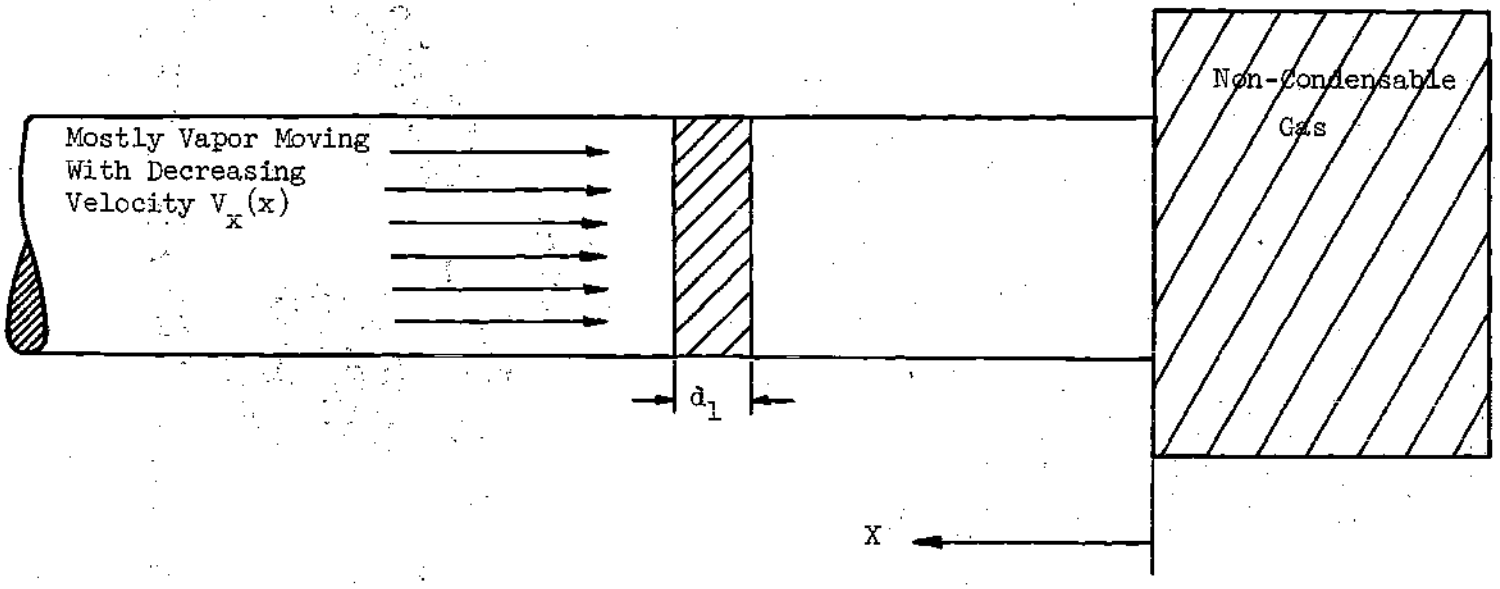

Figure 33. Decreasing Velocity Model.

concentration of non-condensable gas exists.

Considering continuity of gas across the small volume shown (36),

$$n_A = \rho D \frac{dW_A}{dx} + W_A(n_A + n_v) \tag{30}$$

For steady state conditions, the net flux of gas is zero. Therefore,

$$n_A = 0 = -\rho D \frac{dW_A}{dx} + W_A n_v, \text{ and}$$

$$\rho D \frac{dW_A}{dx} - W_A n_v = 0 \tag{31}$$

But $n_v = \rho W_v V_x$, therefore,

$$W_A' + \frac{V_x W_v}{D} W_A = 0 \tag{32}$$

It is now assumed that W_v and D remain fairly constant, since it is presuposed that the flowing mixture contains mostly vapor and that the total pressure and temperature vary only slightly in the axial direction. The axial velocity v_x is assumed to decrease linearly, since this seems to be the case in the condenser section of a heat pipe (26).

Therefore, the term $V_x W_v/D$ can be expressed as

$$\frac{V_x W_v}{D} = K_1 x + K_2$$

But the velocity goes to zero at the interface, which means $K_2 = 0$. Consequently, equation (32) may be written as

$$W_A' + K_1 x W_A = 0 \tag{33}$$

with the boundary condition $W_A(0) = W_{Ao}$.

The solution of equation (33) is

$$\frac{W_A}{W_{Ao}} = \exp\left(-\frac{K_1}{2}x^2\right) \tag{34}$$

To obtain K_1, another value of $\frac{V_x W_v}{D}$ for a particular x must be obtained. In the heat pipe used in this project such a value may be found at the entrance to the condenser, that is at x = 0.5 ft. The values of V_x and D can be obtained as explained previously, for the operating point

P_i = 1.522 in. of Hg; t_{ad} = 150°F.

V_x = 6.762 ft/sec

D = 1.25 x 10^{-3} ft^2/sec

To obtain an approximate value for w_v, the experimental data can be used with the assumption that both the vapor and the gas behave like ideal gases. This assumption is not bad considering the low pressures involved. The vapor concentration can be expressed as

$$W_v = \frac{\rho_v}{\rho_A + \rho_v} = \frac{P_v/R_v T_{ad}}{\frac{P_{nc}}{R_{nc}T_{ad}} + \frac{P_v}{R_v T_{ad}}} = \frac{P_v}{P_{nc}\frac{R_v}{R_{nc}} + P_v} \tag{35}$$

$$W_v = \frac{P_v}{(P_t - P_v)\frac{R_v}{R_{nc}} + P_v} \tag{36}$$

Substituting values from the experimental data it is found that W_v is of the order of 0.80. Therefore,

$$\frac{v_x W_v}{D}\Big| x = 0.5 \text{ ft} = 4.33 \times 10^3 \text{ ft}^{-1}$$

and K_1 is obtained from equation (34) and found to be $K_1 = 8.66 \times 10^3 ft^{-2}$, and therefore the solution of equation (34) is

$$\frac{W_A}{W_{Ao}} = \exp(-4330\, x^2) \tag{37}$$

The value of x for which $\frac{W_A}{W_{Ao}} = 0.01$ is found to be $x_{0.01} = 0.0326$ ft = 0.391 in. indicating that the concentration decreases to a very small value at a very short distance from x = 0.

From the analyses of these two simple systems it may be concluded that, for the tests run in this project, the tendency of the gas to back-diffuse is counteracted by a much larger convective force, such that once the non-condensable gas has accumulated in the condenser end of the heat pipe, it will not back-diffuse, but will remain at that end, as long as the heat pipe is in operation.

The next step will be that of locating the position of the interface between the non-condensable gas and the vapor and to show graphically how the concentration varies with x for different operating conditions. Assume:

1) The interface is perpendicular to the pipe axis.
2) Uniform pressure in the vapor space
3) Uniform non-condensable temperature, equal to T_{ad}.

At operating conditions (see Figure 34),

$$P_{nc} V_{nc} = m_A R_{nc} T_{nc}, \text{ or}$$

$$P_{nc} (\pi r_i^2 L_A) = m_A R_{nc} T_{nc}, \text{ and}$$

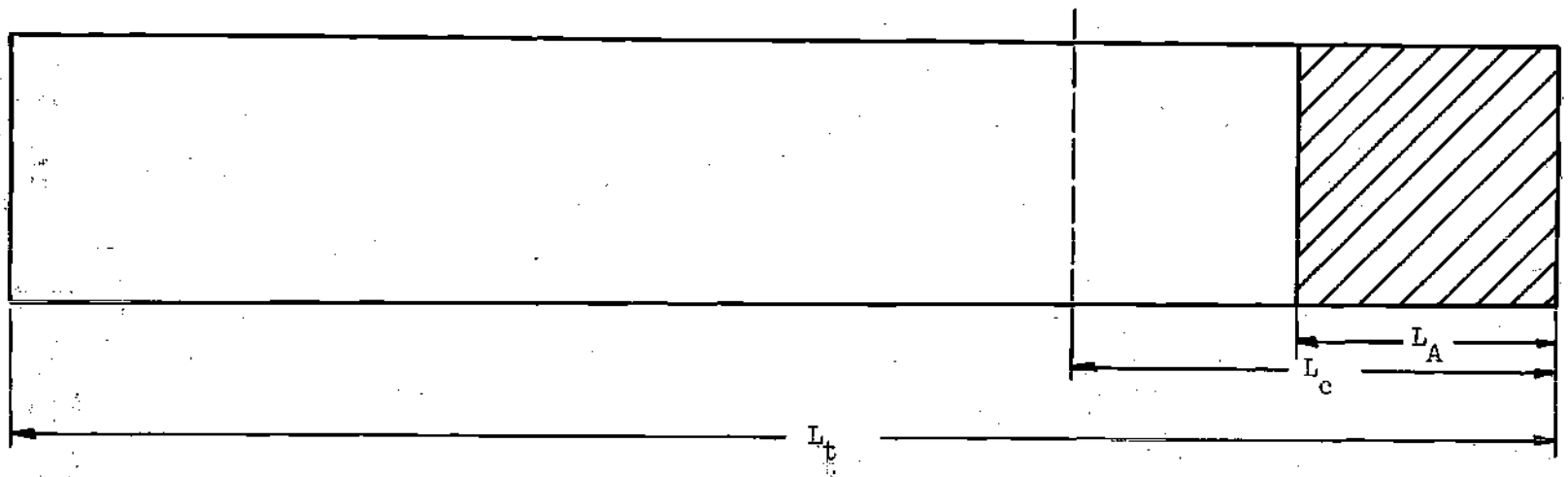

Figure 34. Non-Condensable Gas Location During Operation.

$$L_A = \frac{m_A R_{nc} T_{nc}}{\pi r_i^2 P_{nc}}$$

But $T_{nc} = T_{ad}$ and $P_{nc} = P_{ad}$. Therefore,

$$L_A = \frac{m_A R_{nc} T_{ad}}{\pi r_i^2 P_{ad}}$$

Before water injection, the gas is evenly distributed inside the heat pipe, and

$$P_i V_t = m_A R_{nc} T_i, \text{ or}$$

$$m_A R_{nc} = \frac{P_i (\pi r_i^2 L_t)}{T_i}$$

Therefore,

$$L_A = \frac{P_i T_{ad}}{T_i P_{ad}} L_t \qquad (38)$$

Figures 35 through 38 show the variations of concentration for various operating conditions. These figures were obtained by using equation (38) to find the location of the interface and superposing on it the Argon concentration decay as predicted by equation (34).

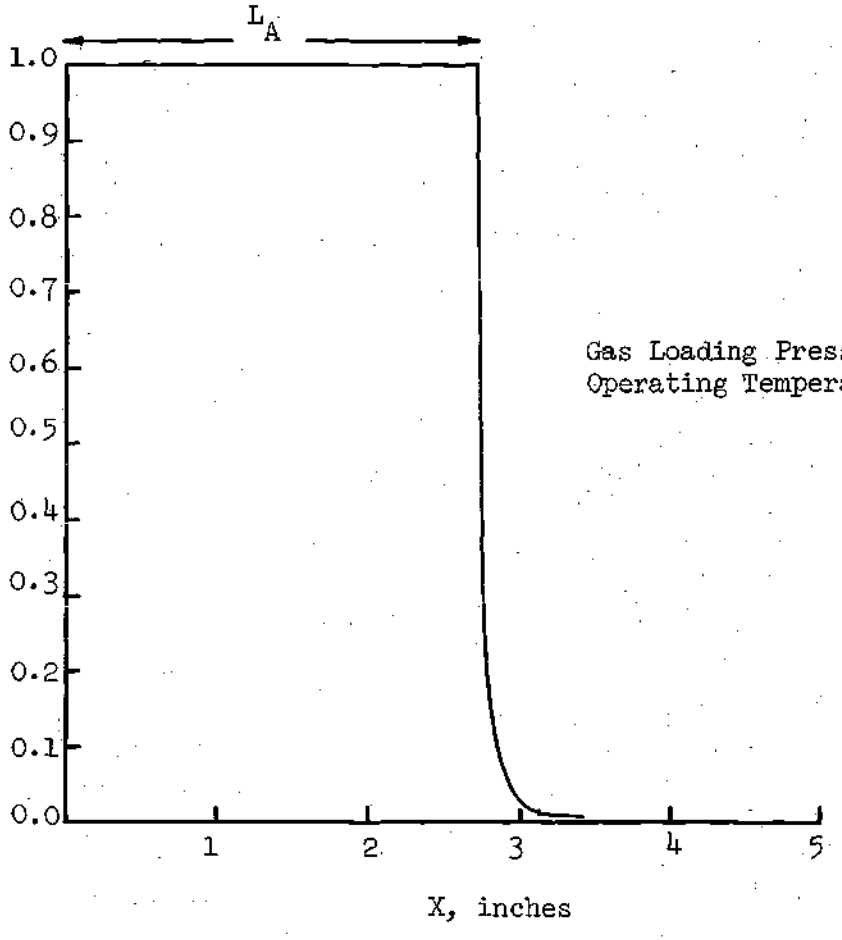

Figure 35. Argon Axial Concentration Profile.

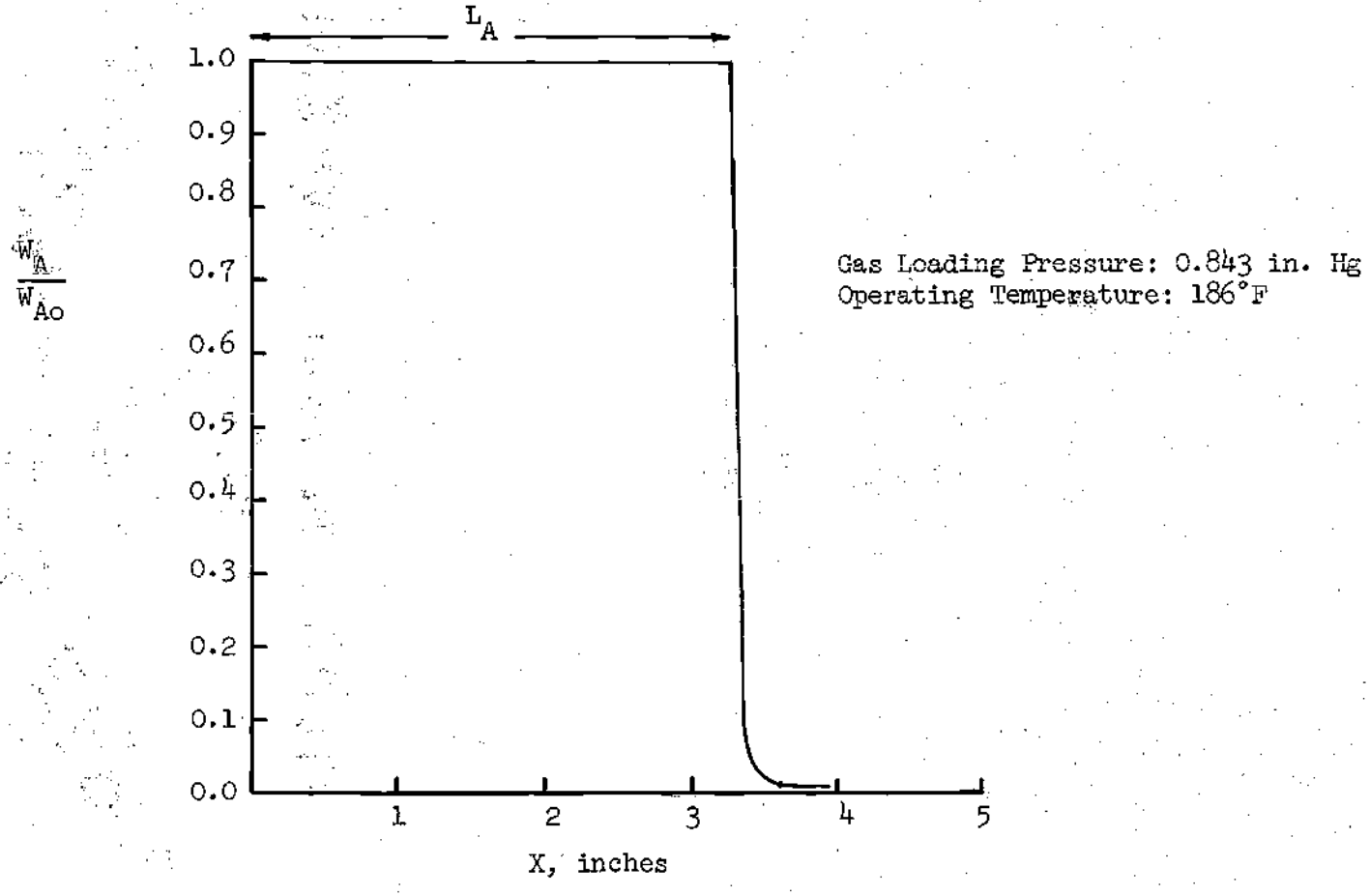

Figure 36. Argon Axial Concentration Profile.

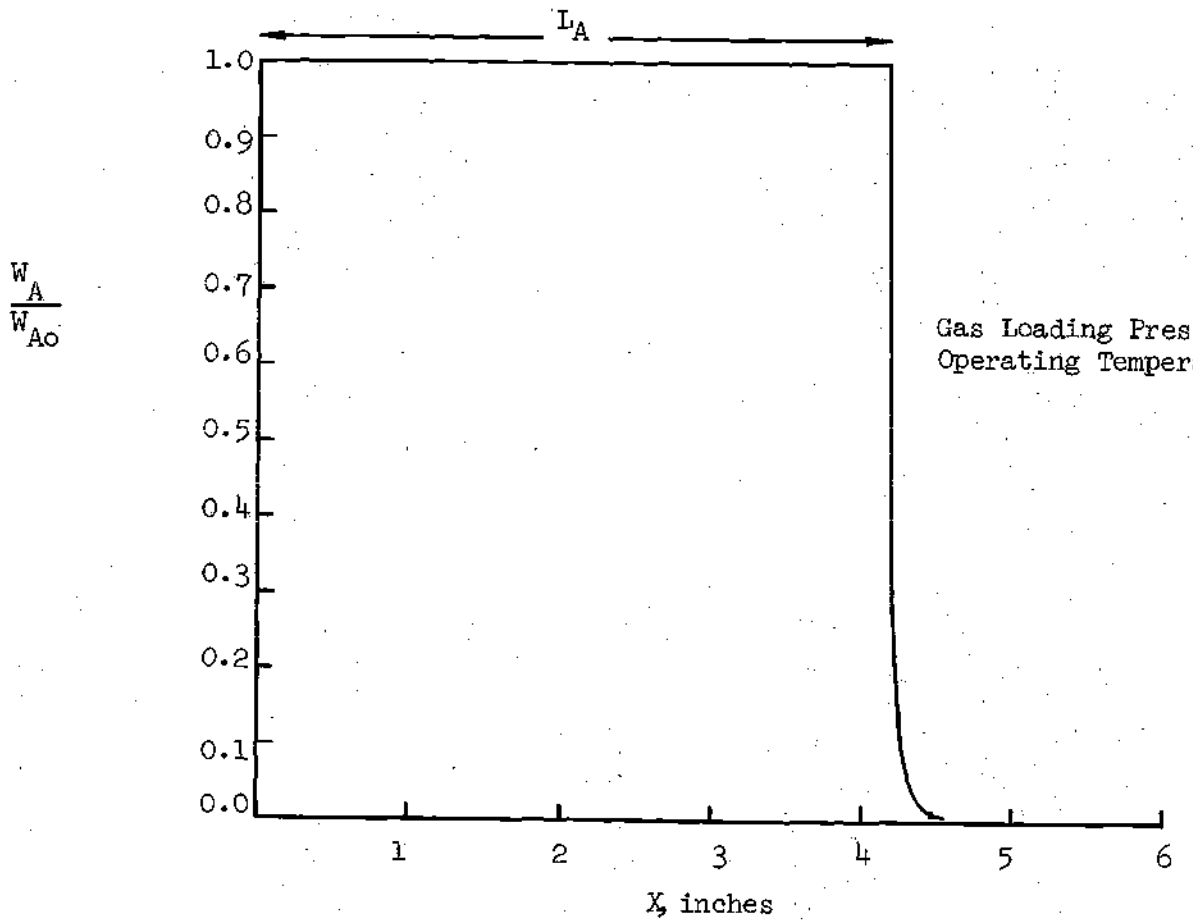

Figure 37. Argon Axial Concentration Profile.

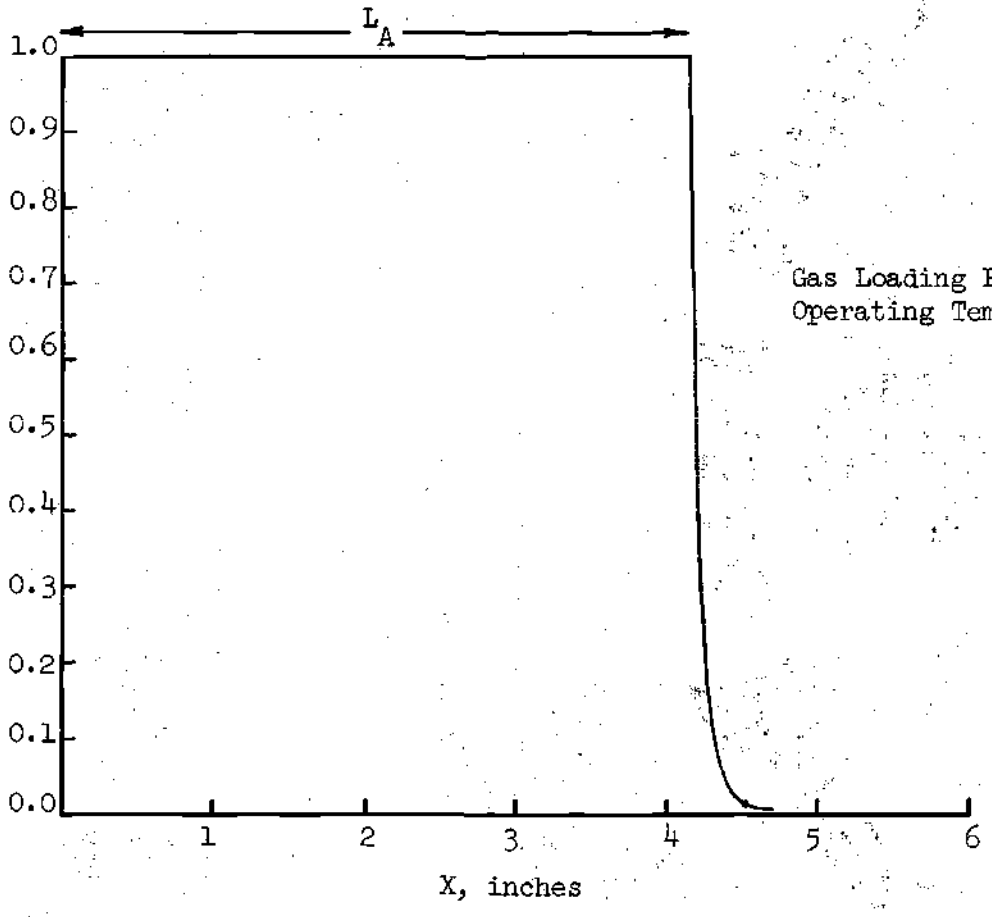

Figure 38. Argon Axial Concentration Profile.

CHAPTER VII

CONCLUSIONS AND RECOMMENDATIONS

The results obtained from this investigation lead to the following conclusions:

1. The performance of a heat pipe can be varied substantially by the inclusion of a non-condensable gas in its vapor space. The rate of heat transfer is decreased proportionally to the amount of non-condensable gas introduced.

2. Though not conclusively shown here, the results strongly indicate that, during operation of the heat pipe, the gas collects at the condenser end forming a slug of gas that effectively reduces the area available for condensation of the working fluid. The position of the interface may be calculated from the operating variables (pressure, temperature, heat pipe dimensions and amount of gas introduced). Thus, the rate of heat transfer for a given operating temperature can be controlled at will, simply by calculating beforehand the necessary amount of a non-condensable gas to be introduced such that the reduction in condenser area will result in the desired reduction in heat transfer.

3. Some generalized heat pipe performance charts can be obtained by use of dimensional analysis. Two such charts are included here. An empirical relation between the non-dimensional variables has been obtained and it approximates the experimental data fairly well.

Obviously, the present investigation is only a small step toward

a better understanding of gas buffered heat pipes. Consequently, the following items are recommended as a logical extension of this investigation:

1. More data is needed in all respects. Different working fluids and non-condensable gases may be used in future studies. With different heating and cooling techniques, the ranges of operation of the heat pipe can be broadened considerably. A wider variation in the amounts of non-condensable gas injected is also needed.

2. Better measurements are necessary to obtain more accurate data. More thermocouples should be placed in the liquid and vapor regions to obtain more information about the operating variables and their influence in heat pipe performance. A better cooling water flow rate measurement device should be used and, if possible, a multiple pass condenser to equalize the axial temperature drop in the condenser region of the heat pipe.

3. A method for tracing the movement and location of the non-condensable gas at various operating conditions must be devised such that the distribution of the gas can be ascertained. Only in this way can the precise location and shape of the interface between the gas and the vapor can be obtained.

4. Other dimensionless groups should be formed and correlations among them obtained over a wide range of operating conditions. In this respect, the use of heat pipes of different geometric characteristics and using various working fluids and non-condensable gases should lead to generalized performance charts.

5. A complete theoretical analysis of non-condensable gas behavior in the heat pipe and its influence in heat pipe performance is needed. The conservation equations for heat, mass and momentum transfer should be used to obtain relations suitable for heat pipe design.

APPENDIX

EXPERIMENTAL DATA

Test No. 9 April 15, 1969

Initial Pressure: 5μ Hg Final Pressure: 6.01 in. Hg
Initial Temperature: 66°F Final Temperature: 64°F
Comments: Runs 1-4 have been deleted, since they were performed before the second water injection.

Run No.	Time of Run Min.	Cooling Water Flow Lts.	Thermocouple Readings T2	T3-T2	T5	T6	T7	Pipe Pressure in.Hg	V volts	Q btu/hr
5	1.5	.770	56	1.6	77	77	83	1.6	20	109
6	1.5	.770	56	1.6	77	77	82	1.6	20	109
7	1.5	.771	56	1.6	77	77	82	1.6	20	110
8	1.5	.774	56	2.9	84	84	92	2.1	31	195
9	1.5	.771	56	2.9	84.5	84.5	94	2.1	31	198
10	1.5	.772	56	2.9	85.5	86	95	2.1	31	205
11	1.5	.772	56	5.2	96	96	116	2.8	41	357
12	1.5	.772	56	5.4	97	97	118	2.8	41	368
13	1.5	.773	56	5.4	98	98	120	2.8	41	370
14	1.5	.773	56	5.4	98.5	98.5	120	2.8	41	370
15	1.5	.773	60	7.0	107.5	108	140	3.9	46	475
16	1.5	.772	60	7.1	108.5	108.5	140.5	4.0	46	484
17	1.5	.772	60	7.1	109	109.5	141	3.9	46	484
18	1.5	.773	60	7.1	109	109.5	141	3.9	46	484
19	1.5	.775	62	8.6	118.5	119	155	4.7	50	585
20	1.5	.774	61.5	8.6	119	119.5	156.5	5.0	50	587
21	1.5	.774	60.5	8.6	119	119.5	156	4.9	50	587
22	1.5	.774	60	10.3	128.5	129.5	168	5.9	55.5	701
23	1.5	.774	60	10.4	128.5	129.5	167.5	5.9	55.5	711
24	1.5	.773	60	10.4	129	130	167.5	5.9	55.5	709
25	1.5	.775	60	10.6	129	130	167.5	6.0	55.5	725
26	1.5	.775	61	13.1	142.5	143.5	182	8.3	60	884
27	1.5	.776	60	12.7	143.5	144	182	8.0	60	873
28	1.5	.774	60	12.7	143.5	144	182	8.6	60	869
29	1.5	.773	62	12.9	144	144	183	8.7	60	882
30	1.5	.772	60	15.1	158	158	199	11.5	65	1030
31	1.5	.771	60	15.1	158.5	160	202	11.8	65	1025
32	1.5	.772	59.5	15.6	164	165	205.5	12.9	65	1065
33	1.5	.772	59	15.6	164	165	207	12.9	65	1065
34	1.5	.771	59	15.6	165	166	209	12.9	65	1064

Test No. 12 May 24, 1969

Initial Pressure: 21,400 μ Hg
Initial Temperature: 63.5°F
Comments: None

Final Pressure: 1.44 in. Hg
Final Temperature: 62.5°F

Run No.	Time of Run Min.	Cooling Water Flow Lts.	Thermocouple Readings T2	T3-T2	T5	T6	T7	Pipe Pressure in.Hg.	V volts	Q btu/hr
1	1.5	.773	66.0	1.05	114.0	114.0	115.0	3.7	21.0	71.5
2	1.5	.774	66.0	1.25	114.0	114	115	3.7	21.0	85.0
3	1.5	.777	66.0	1.20	114.0	114	116	3.7	21.0	82.1
4	1.5	.776	66.0	1.20	114.5	114.5	117	3.7	21.0	82.2
5	1.5	.774	63.0	2.45	118.0	118	123	4.0	30.0	168
6	1.5	.777	63.0	2.45	118.5	118.5	124	4.4	30.0	168
7	1.5	.773	63.0	2.48	119.0	119	125	4.8	30.0	169
8	1.5	.776	66.5	4.75	126.0	126.5	148	5.0	40.5	291
9	1.5	.775	66.5	4.81	126.0	126.5	149	5.0	40.5	330
10	1.5	.776	66.5	4.85	126.5	127	151	5.0	40.5	332
11	1.5	.774	66.5	4.90	126.5	127	152	5.1	40.5	334
12	1.5	.775	67.0	6.30	131.0	131.5	167	5.9	45	431
13	1.5	.776	67.0	6.40	130.5	131.5	167	5.9	45	438
14	1.5	.775	67.0	6.40	130.5	131.5	167.5	6.1	45	438
15	1.5	.774	67.5	8.00	136.0	137	177.5	6.5	50.5	547
16	1.5	.775	67.5	8.10	136.0	137	180	6.5	50.5	554
17	1.5	.775	67.0	8.20	136.0	137.5	181.5	6.5	50.5	560
18	1.5	.776	67.0	9.80	143	144	195	7.7	54.5	672
19	1.5	.778	67.0	9.80	143	144	197	7.8	55	673
20	1.5	.778	66.7	9.81	143	144	198	7.8	55	673
21	1.5	.778	67.5	12.2	150.5	152	212	9.5	59.8	836
22	1.5	.777	67.0	12.1	151.0	152.5	215	9.7	59.8	830
23	1.5	.777	66.0	12.0	151.5	153.5	217	9.9	59.8	837
24	1.5	.776	66.5	15.1	164.0	166	238.5	13.4	66	1030
25	1.5	.778	66.0	15.8	168.0	170	245	14.6	66	1079
26	1.5	.777	66.0	15.8	169.5	171.5	246	14.9	66	1085
27	1.5	.779	65.0	15.9	170.0	172	246.5	15.2	66	1090

Test No. 13

May 28, 1969

Initial Pressure: 11,320 μ Hg
Initial Temperature: 62.5°F
Comments: None

Final Pressure: 1.0 in. Hg
Final Temperature: 62°F

Run No.	Time of Run Min.	Cooling Water Flow Lts.	Thermocouple Readings T2	T3-T2	T5	T6	T7	Pipe Pressure in.Hg	V volts	Q $\frac{btu}{hr}$
1	1.5	.774	64.0	0.90	95.0	95.2	98.3	2.0	20	61.5
2	1.5	.775	64.0	1.02	96.0	96	99.5	2.2	20	69.9
3	1.5	.772	64.0	1.1	96.0	96	99.5	2.4	20	75
4	1.5	.772	64.5	1.1	96	96	100	2.5	20	75
5	1.5	.772	64	1.2	96	96.5	100	2.5	20	81.7
6	1.5	.772	64	1.2	96	96	105	2.4	20	81.7
7	1.5	.772	64.5	2.42	103	103	110.5	2.9	30	165
8	1.5	.772	64.5	2.67	103	103	112	2.9	30	183
9	1.5	.777	64.6	2.67	103	103.5	112	2.9	30	178
10	1.5	.772	64.6	2.72	104	104	114	2.9	30	186
11	1.5	.771	64	4.61	110.5	110.5	133	3.7	40	314
12	1.5	.775	64.2	4.75	111	111.5	135	3.7	40	325
13	1.5	.772	64.5	4.95	112	112	137	3.9	40	342
14	1.5	.774	64.6	4.92	112.2	112.8	138.5	3.9	40	337
15	1.5	.774	64.6	6.1	117	117.5	150	4.6	45.5	417
16	1.5	.775	64.5	6.21	118	118	152	4.6	45.5	425
17	1.5	.776	64.5	6.31	118.5	118.5	153	4.6	45.5	438
18	1.5	.775	64.8	7.88	124	124	167	5.3	50	535
19	1.5	.776	64.5	8.0	124	124	168	5.3	50	549
20	1.5	.776	64.2	8.0	124	124.5	169	5.3	50	549
21	1.5	.776	64.2	8.0	124	124	170	5.5	50	549
22	1.5	.777	64.2	9.66	132	132	185.5	6.3	54.6	664
23	1.5	.777	64	9.7	132	132.6	186	6.3	55	675
24	1.5	.775	64	9.8	132.5	133.5	188	6.4	55	672
25	1.5	.775	64	9.8	133	135.5	189	6.4	55	672
26	1.5	.777	66.5	11.3	143.5	144.5	208	8.6	60	776
27	1.5	.776	65.5	12.28	144.5	145.5	208	8.6	60	842
28	1.5	.778	65	12.4	145	146	208	9.0	60	852
29	1.5	.775	66.5	12.62	147	148	210	9.5	60	865
30	1.5	.778	64	14.8	158	159.5	224	11.7	65	1016
31	1.5	.779	65	15.0	159	160	225	12.2	65	1032
32	1.5	.779	66.5	14.9	160	160	227	12.2	65	1025
33	1.5	.778	64	14.85	159	160	225	12.4	65	1020

Test No. 14 July 10, 1969

Initial Pressure: 38,700 μ Hg
Initial Temperature: 70.5°F
Comments: None

Final Pressure: 2.07 in. Hg
Final Temperature: 69°F

Run No.	Time of Run Min.	Cooling Water Flow Lts.	Thermocouple Readings T2	T3-T2	T5	T6	T7	Pipe Pressure in.Hg	V volts	Q btu/hr
1	1.5	.774	70.5	0.94	128.5	129	130	4.7	20	61.7
2	1.5	.770	70.0	0.94	128.5	129	130.5	4.8	20	58.1
3	1.5	.774	70.5	1.00	128.5	129	130.5	4.8	20	65.7
4	1.5	.770	70.0	1.05	128.5	129	131	4.7	20	71.5
5	1.5	.771	70.5	1.10	129	129	130.5	4.5	20	74.9
6	1.5	.773	71	2.75	133.5	134	143	5.6	30	187
7	1.5	.771	71	2.75	134	134	142.5	5.5	30	187
8	1.5	.771	71	2.75	133.5	134	142.5	5.5	30	187
9	1.5	.774	72.5	5.15	142	142	164	6.9	40	352
10	1.5	.772	72.5	5.15	143	143	165	6.9	40	351
11	1.5	.774	73	5.5	142	142.5	165.5	6.9	40	352
12	1.5	.773	73	6.55	146	146.5	175	7.1	45.5	446
13	1.5	.773	73	6.55	146	146.5	174	7.6	45.5	446
14	1.5	.775	73	6.60	146	146.5	174.5	7.6	45.5	451
15	1.5	.774	73	8.05	150	150.5	181.5	8.4	50	550
16	1.5	.774	72.5	8.10	150	151	182	8.5	50	554
17	1.5	.774	72.5	8.12	150	151	182	8.4	50	555
18	1.5	.774	70	10.1	156.5	157	190	9.8	54.5	690
19	1.5	.774	70	10.0	156.5	157	192	9.9	54.5	684
20	1.5	.774	70	10.0	156.5	157	193	9.9	54.5	684
21	1.5	.775	69.0	12.6	164.0	164.5	206	11.8	60	862
22	1.5	.774	69.5	12.6	164.5	164.5	206	12.1	60	861
23	1.5	.774	69.5	12.7	164.5	164.5	205	12.2	60.5	868
24	1.5	.776	67.0	15.65	175.5	176	225	15.6	65.5	1072
25	1.5	.777	67.0	15.65	174	175	223.5	15.2	65.5	1072
26	1.5	.779	65.0	17.0	178.5	178.5	231	17.3	67.5	1169
27	1.5	.780	65.0	16.0	178.5	178.5	234.5	17.1	67.5	1170

Test No. 16 July 22, 1969

Initial Pressure: 50,820 μ Hg Final Pressure: 2.4 in. Hg
Initial Temperature: 73°F Final Temperature: 68°F
Comments: None

Run No.	Time of Run Min.	Cooling Water Flow Lts.	Thermocouple Readings T2	T3-T2	T5	T6	T7	Pipe Pressure in.Hg	V volts	Q btu/hr
1	1.5	.777	73.5	0.78	135	135	136	6.3	20	53.5
2	1.5	.775	73.5	0.80	135	135	136	6.1	20	54.8
3	1.5	.777	73.5	0.80	135	135	136.5	6.1	20	54.9
4	1.5	.772	73.5	2.35	140	140	144	6.0	30	160.2
5	1.5	.773	73.5	2.38	140	140	144.5	6.0	30	162.4
6	1.5	.775	73.5	2.50	140	140	145.5	6.0	30	171
7	1.5	.773	73.5	2.50	140.5	140.5	146	6.0	30	171
8	1.5	.775	73.5	2.50	140	140	145	6.0	30	171
9	1.5	.773	73.5	4.55	147	147	157.5	7.7	40	311
10	1.5	.775	73.5	4.70	146.5	147	158	7.8	40	321
11	1.5	.774	73.0	4.70	147	147	159	7.9	40	321
12	1.5	.774	73.5	6.20	151	151	169.5	8.1	45.5	424
13	1.5	.775	73.5	6.20	151	151	170	8.8	45.5	424
14	1.5	.775	73.5	7.95	155.5	155.5	179.5	9.9	50	544
15	1.5	.777	73.5	7.90	155.5	155.5	179	10.0	50	542
16	1.5	.776	73.5	7.95	155.0	155.5	179.5	10.1	50	544
17	1.5	.776	74.0	9.70	161.5	162.5	189.5	11.9	55.8	665
18	1.5	.776	74.0	10.0	161.5	162.5	189.5	12.0	55.5	689
19	1.5	.776	74.5	9.95	161.5	162	190	12.0	55.5	683
20	1.5	.776	74.0	10.0	161.5	162.5	192	12.1	55.5	686
21	1.5	.777	74.5	12.3	167	168	206	14.0	60.0	845
22	1.5	.779	74.5	12.2	167	169	206.5	14.0	59.5	838
23	1.5	.774	74.0	12.1	167.3	169	208	13.9	59.5	826
24	1.5	.778	74.0	12.2	167	168.5	208	14.0	59.5	838
25	1.5	.777	73.5	15.3	176	178	226	17.8	66.0	1050
26	1.5	.779	73.5	15.4	176.5	178	226.5	18.2	65.5	1060
27	1.5	.780	73.5	15.2	177	179	227.5	18.0	65.0	1049
28	1.5	.777	73.0	17.2	183	184	240.5	19.4	68.0	1170
29	1.5	.779	73.0	17.2	188	189	245	21.1	68.0	1181
30	1.5	.781	73.0	17.5	184	186	244.5	20.3	68.5	1203
31	1.5	.779	73.0	17.4	184.5	186	243	20.5	68.5	1195

LITERATURE CITED

1. L. G. Neal, An Analytical and Experimental Study of Heat Pipes, Independent Research Report, TRVV Systems, Redondo Beach, California, January 1967.

2. K. T. Feldman, Jr. and G. H. Whiting, "Applications of the Heat Pipe," Mechanical Engineering (Nov. 1968).

3. G. H. Parker and J. P. Hanson, "Heat Pipe Analysis," Intersociety Energy Conversion Engineering Conference, Miami, 1967.

4. G. Wener and D. Lee, Concept for a Gas Buffered Annular Heat Pipe Fuel. Irradiation Capsule, Lawrence Radiation Laboratory, Livermore, Report UCRL-50510, July 1968.

5. R. Gaugler, "Heat Transfer Device." U. S. Patent 2, 350, 348, June 6, 1944.

6. G. M. Grover, T. P. Cotter, and G. F. Erickson, "Structures of Very High Thermal Conductances." J. App. Phys. 35, 1990 (1964).

7. T. P. Cotter, Theory of Heat Pipes, Los Alamos Scientific Laboratory Report LA-3246-MS, March 1965.

8. J. H. Cosgrove, Engineering Design of the Heat Pipe, PhD Thesis, North Carolina State University, 1967.

9. E. K. Levy, "Theoretical Investigation of Heat Pipes Operating at Low Vapor Pressures," Journal of Engineering for Industry, Transactions of the ASME, Nov. 1968.

10. H. R. Kunz, S. S. Wyde, G. H. Nashick, and J. F. Barnes, Vapor-Chamber Fin Studies, Operating Characteristics of Fin Models, Pratt and Whitney Aircraft Report NASA Cr-1139, August 1968.

11. P. Brosens, "Thermionic Converters with Heat Pipe Radiators," Intersociety Energy Conversion Engineering Conference, Miami, 1967.

12. J. Deverall and J. Kemme, High Thermal Conductance Devices Utilizing the Boiling of Lithium and Silver, Los Alamos Scientific Laboratory Report LA-3211, 1965.

13. J. E. Kemme, "Heat Pipe Capability Experiments," Proceedings of Joint Atomic Energy Commission/Sandia Laboratories Heat Pipe Conference, Volume I, October 1966.

LITERATURE CITED (Continued)

14. L. S. Langston and H. R. Kunz, Liquid Transport Properties of Some Heat Pipe Wicking Materials, ASME Publication 69-HT-17.

15. J. C. Chato and J. H. Streckert, Performance of a Wick-Limited Heat Pipe, ASME Publication 69-HT-20.

16. S. Frank "Optimization of a Grooved Heat Pipe," Intersociety Energy Conversion Engineering Conference, Miami, 1967.

17. J. H. Cosgrove, J. K. Ferrell, and A. Carnesale, "Operating Characteristics of Capillarity Limited Heat Pipes," J. Nuclear Energy 21, 1967.

18. E. C. Phillips and J. D. Hinderman, Determination ofProperties of Capillary Media Useful in Heat Pipe Design, ASME Puvlication 69-HT-18.

19. D. K. Anand, A. Z. Dybbs, and R. E. Jenkins, "Effects of Condenser Parameters on Heat Pipe Optimization," J. Spacecraft, Vol. 4, No. 5, May 1967.

20. H. R. Kunz, L. S. Langston, B. H. Hilton, S. S. Wyde, and G. H. Nashick, Vapor-Chamber Fin Studies, Transport Properties and Boiling Characteristics of Wicks, Pratt and Whitney Airfraft Report NASA CR-812, June 1967.

21. P. J. Marto and W. L. Mosteller, Effect of Nucleate Boiling on the Operation of Low Temperature Heat Pipes, ASME Publication 69-HT-24.

22. T. I. McSweeney, "The Performance of a Sodium Heat Pipe," presented at the Eleventh National Heat Transfer Conference A.I.Ch.E. - A.S.M.E., Minneapolis, Minnesota, August 1969.

23. F. A. Lyman and Y. S. Huang, Analysis of Temperature Distributions in Heat Pipe Wicks, ASME Publication 69-HT-23.

24. E. Schmidt, Contribution a L'Etude des Caloducs, Theses Presentees a la Faculte des Sciences de L'Universite de Grenoble pour obtenir le Grade de Docteur-Ingenieur, Grenoble, 1968.

25. G. S. Dzakowic, Y. S. Tang, and F. G. Arcella, Experimental Study of Vapor Velocity Limit in a Sodium Heat Pipe, ASME Publication 69-HT-21.

26. L. S. Galowin and V. A. Barker, Heat Pipe Channel Flow Distributions, ASME Publication 69-HT-22.

LITERATURE CITED (Concluded)

27. H. C. Haller and S. Lieblien, "Feasibility Studies of Space Radiators Using Vapor Chamber Fins," Proceedings of Joint Atomic Energy Commission/Sandia Laboratories Heat Pipe Conference, Volume I, October 1966.

28. S. Katzoff, "Notes on Heat Pipes and Vapor Chambers and their Application to Thermal Control of Spacecraft," Proceedings of Joint Atomic Energy Commission/Sandia Laboratories Heat Pipe Conference, Volume I, October 1966.

29. J. E. Deverall and J. E. Kemme, Satellite Heat Pipe, Los Alamos Scientific Laboratory Report LA-3278-MS, January 1965.

30. C. C. Silverstein, Heat Pipe Gas Turbine Regenerators, ASME Publication 68-WA/GT-7.

31. T. P. Cotter, "Heat Pipe Startup Dynamics," Thermionic Conversion Specialist Conference, Palo Alto, 1967.

32. J. Schwartz, Performance Map of the Water Heat Pipe and the Phenomenon of Noncondensible Gas Generation, ASME Publication 69-HT-15.

33. R. Wener, The Generation and Recovery of Tritium in Thermonuclear Reactor Blankets Using Heat Pipes, Lawrence Radiation Laboratory, Livermore, Report UCID-15390, October 1968.

34. _____, Tables of Thermal Properties of Gases, National Bureau of Standards Circular 564.

35. H. Hampson, "The Condensation of Steam on a Tube with Filmwise or Dropwise Condensation and in the Presence of a Non-Condensable Gas," International Developments in Heat Transfer, Proceedings of 1961-1962 International Heat Transfer Conference, ASME, 1963.

36. R. Bird, W. Stewart, E. Lightfoot, Transport Phenomena (John Wiley and Sons, New York, 1966), 7th Printing.

Other References

_____, 1967 ASME Steam Tables, Thermodynamic and Transport Properties of Steam (The American Society of Mechanical Engineers, New York, 1968) 2nd Edition.

Keenan, J. F. and Keyes, F. G. Thermodynamic Properties of Steam (John Wiley and Sons, New York, 1964), 36th Printing.

Kreith, F., Principles of Heat Transfer (International Textbook Co., Scranton, Pennsylvania, 1966), 2nd Printing.

Van Wylen, J. G. and Sonntag, R. F., Fundamentals of Classical Thermodynamics (John Wiley and Sons, New York, 1966), 2nd Printing.